RECOVERY OF INDUSTRIAL ANNEALING FURNACE WASTE HEAT USING COMBINED SYSTEMS AND THERMOECONOMIC ANALYSIS

2021
MASTER THESIS
MECHANICAL ENGINEERING

Büşra TOM

RECOVERY OF INDUSTRIAL ANNEALING FURNACE WASTE HEAT USING COMBINED SYSTEMS AND THERMOECONOMIC ANALYSIS

BÜŞRA TOM

T.C.
Karabük University
Institute of Graduate Programs
Department of Mechanical Engineering
Prepared as
Master Thesis

Assist. Prof. Dr. Erhan KAYABAŞI

KARABUK
JUNE 2021

I certify that in my opinion the thesis submitted by Büşra TOM titled "RECOVERY OF INDUSTRIAL ANNEALING FURNACE WASTE HEAT USING COMBINED SYSTEMS AND THERMOECONOMIC ANALYSIS" is fully adequate in scope and in quality as a thesis for the degree of Master of Science.

Assist. Prof. Dr. Erhan KAYABAŞI ……
Thesis Advisor, Department of Mechanical Engineering

This thesis is accepted by the examining committee with a unanimous vote in the Department of Mechanical Engineering as a Master of Science. June 07, 2021.

Examining Committee Members (Institutions)	Signature
Chairman: Prof. Dr. Kamil ARSLAN (KBU)	……
Member : Assist. Prof. Dr. Erhan KAYABAŞI (KBU)	……
Member : Assist. Prof. Dr. Fatih UYSAL (SUBU)	……

The degree of Master of Science by the thesis submitted is approved by the Administrative Board of the Institute of Graduate Programs, Karabük University.

Prof. Dr. Hasan SOLMAZ ……
Director of the Institute of Graduate Programs

"I declare that all the information within this thesis has been gathered and presented in accordance with academic regulations and ethical principles and I have according to the requirements of these regulations and principles cited all those which do not originate in this work as well."

Büşra TOM

ABSTRACT

M. Sc. Thesis

RECOVERY OF INDUSTRIAL ANNEALING FURNACE WASTE HEAT USING COMBINED SYSTEMS AND THERMOECONOMIC ANALYSIS

Büşra TOM

Karabuk University
Institute of Graduate Programs
The Department of Mechanical Engineering

Thesis Advisor:
Assist. Prof. Dr. Erhan KAYABAŞI
June 2021, 56 pages

Increasing energy demand and cost, decreasing energy resources and environmental factors require efficient use of energy. In this context, it is aimed to recover the waste heat of industrial annealing furnace with various energy conversion methods in this study. In the study, the flue gas of the annealing furnace at 1093.15 K was evaluated with four different combined systems. These combinations have been studied parametrically. Thermodynamics and thermoeconomic analysis were performed for each combined system using the Engineering Equation Solver (EES). And the using waste heat recovery systems (WHRS) examined the environmental effect. All combined systems are compared with each other in terms of thermal efficiency, net power output and electricity generation cost. As a result of the parametric study, the lowest electricity production cost, net power output and thermal efficiency 0.01153 $/kWh, 1274 kW and 0.36 from *SRC-CO_2* combined system, respectively. The net power from highest to lowest are 1274 kW (*SRC-CO_2*), 1010 kW (*SRC-ORC-KC*),

935.6 kW (*KC-CO_2*) and 766.2 kW (*SRC-ORC-KC*) when the powers from the combined cycles are compared with each other. The electricity generation cost from lowest to highest are 0.01153 $/kWh (*SRC-$CO_2$*), 0.01534 $/kWh (*ORC-$CO_2$*), 0.01706 $/kWh (*SRC-ORC-KC*) and 0.08427 $/kWh (*KC*-$CO_2$) when the electricity generation cost from the combined system are compared with each other. The thermal efficiency from highest to lowest are 0.44 (*SRC-ORC-KC*), 0.36 (*SRC-CO_2*) 0.26 (*KC-CO_2)* and 0.21 (*SRC-ORC-KC*) when the thermal efficiency from the combined cycles are compared each other.

Key Words : Waste heat recovery, environmental impact, thermoeconomic analysis, Steam Rankine Cycle (SRC), CO_2 cycle, Organic Rankine Cycle (ORC), Kalina cycle (K.C.)

Science Code : 91408

ÖZET

Yüksek Lisans Tezi

ENDÜSTRİYEL TAV FIRINI ATIK ISISININ KOMBİNE SİSTEMLER KULLANILARAK GERİ KAZANIMI VE TERMOEKONOMİK ANALİZİ

Büşra TOM

Karabük Üniversitesi
Lisansüstü Eğitim Enstitüsü
Makine Mühendisliği Anabilim Dalı

Tez Danışmanı:
Dr. Öğr. Üyesi Erhan KAYABAŞI
Haziran 2021, 56 sayfa

Artan enerji talebi ve maliyeti, azalan enerji kaynakları ve çevresel faktörler, enerjinin verimli kullanılmasını gerektirmektedir. Bu kapsamda bu çalışmada endüstriyel tavlama fırınının atık ısısının çeşitli enerji dönüşüm yöntemleri ile geri kazanılması amaçlanmaktadır. Çalışmada 1093,15 K sıcaklıktaki tavlama fırınının baca gazı, dört farklı kombine sistem ile değerlendirilmiştir. Bu kombine çevrimler parametrik olarak incelenmiştir. Mühendislik Denklem Çözücü (EES) kullanılarak her bir kombine sistem için termodinamik ve termoekonomik analizler yapılmıştır. Atık ısı geri kazanım sistemlerinin kullanılması ve çevreye etkisi incelenmiştir. Tüm kombine sistemler, termal verimlilik, net güç çıkışı ve elektrik üretim maliyeti açısından birbirleriyle karşılaştırılmıştır. Parametrik çalışma sonucunda en düşük elektrik üretim maliyeti, net güç çıkışı ve termal verim 0,01153 $/kWh, 1274 kW ve 0,36 *SRC-CO_2* kombine sisteminden elde edilmiştir. Kombine çevrimlerden elde edilen güçler birbirleriyle karşılaştırıldığında en yüksek değerden en düşük değere net güç 1274 kW

(*SRC-CO_2*), 1010 kW (*SRC-ORC-KC*), 935,6 kW (*KC-CO_2*) ve 766,2 kW (*ORC-CO_2*)'tır. Kombine çevrimlerden elde edilen elektrik üretim maliyetleri birbirleriyle karşılaştırıldığında en düşük değerden en yüksek değere 0,01153 $/kWh (*SRC-$CO_2$*), 0,01534 $/kWh (*ORC-$CO_2$*), 0,01706 $/kWh (*SRC-ORC-KC*) ve 0,08427 $/kWh (*KC-$CO_2$*)tir. Kombine çevrimlerin ısıl verimleri karşılaştırıldığında en yüksek değerden en düşük değere doğru ısıl verim 0,44 (*SRC-CO_2*), 0,36 (*SRC-ORC-KC*), 0,26 (*KC-CO_2*) ve 0,21 (*ORC-CO_2*)'dir.

Anahtar Kelimeler : Atık ısı geri kazanımı, çevresel etki, termoekonomik analizler, Buhar Rankine Çevrimi, Organik Rankine Çevrimi, Kalina Çevrimi, CO_2 Çevrimi.

Bilim Kodu **:** 91408

ACKNOWLEDGEMENT

I would like to thank my supervisor Assist. Prof. Dr. Erhan KAYABAŞI, who did not spare his precious time, knowledge, and experience during the process from the formation of my thesis study to its completion.

I also present my thanks to Assoc. Dr. Hasan ÖZCAN, who assisted me with my theoretical studies. On the other hand, I would like to thank Assist. Prof. Dr. Enes KILINÇ and Res. Assist. Mutlucan BAYAT for helping me in this thesis process. We are grateful to Karabük University for providing its software and hardware infrastructure to realize the current study.

I want to thank my dear family and Muhammet BEŞEVLİ, who did not spare any moral support.

CONTENTS

Page

Page

LIST OF FIGURES

Page

LIST OF TABLES

Page

SYMBOLS AND ABBREVIATIONS INDEX

SYMBOLS

A	: area, m^2
Cp	: specific heat, kJ/kgK
CRF	: capital recovery factor, dimensionless
Ɛ	: effectiveness, dimensionless
ί	: annual interest rate, %
N	: annual operating hours, h
n	: system lifetime, y
ρ	: density, kg/m^3
Ż	: capital cost rate, $/s
Z	: capital cost, $
η	: efficiency
ϕ	: maintenance factor, dimensionless
x	: ammonia fraction, %

SUBSCRIPTS

fg	: flue gas
cc	: combined cycle
p	: pump
t	: turbine
hex	: heat exchanger
cw	: cooling water
gen	: generator
cond	: condenser
eva	: evaporator
ST	: steam turbine

RHE : recovery heat exchanger

mx : mixer

s : seperator

HTR : high temperature recuperator

LTR : low temperature recuperator

exp : expansion valve

ABBREVIATIONS

SRC : Steam Rankine Cycle

ORC : Organic Rankine Cycle

CO_2 : Carbon Dioxide

KC : Kalina Cycle

HFG : High Furnace Gas

DARS : Double-effect Absorption Refrigeration System

HT : High Temperature

LT : Low Temperature

ARS : Absorption Refrigeration System

VCHP : Vapor Compression Heat Pump

1AHP : First Absorption Heat Pump

2AHP : Second Absorption Heat Pump

DH : Direct Heating

COP : Coefficient of Performance

GHG : Green House Gas

GT : Gas Turbine

PEC : Purchased Equipment Cost

EES : Engineering Equation Solver

SH : Sensible Heat

NH_3H_2O : Ammonia-water mixture

WHRS : Waste Heat Recovery Systems

WHR : Waste Heat Recovery

TIT : Turbine inlet temperature

AWM : Ammonia-water mixture

SECTION 1

INTRODUCTION

Energy is of paramount importance for social development, economical and quality of life in all countries [1]. Energy is used in all areas of life; It has various mechanical, thermal, geothermal, biomass, solar, chemical, nuclear, wind and electrical power. These energies can be converted into each other by appropriate processes [2].

Energy resources are renewable and non-renewable in terms of their use; they are classified as primary and secondary energy resources in their transformation capabilities [3]. Producing and using energy efficiency has become a worldwide problem [4]. The need for energy more and more day by day, together with the limited energy resources of the world and its continuous decrease, has led countries to reconsider their energy policies and to use energy efficiently [2].

In scientific circles, it tries to re-evaluate energy transformation tools and develop new methods to benefit more from the limited energy resources available [2]. One of the most critical challenges faced by engineers is to design efficient systems that have low investment and operating costs and, at the same time, do not negatively affect the environment. In addition, global warming, ozone depletion and CO_2 emissions are increasing significantly as environmental problems. The flue gas resulting from industrial processes is the primary source of CO_2 emission. CO_2, which constitutes approximately 68% of greenhouse gases and is one of the components of flue gases, causes global warming and climate change [5].

Figure 1.1 shows the total amount of CO_2 emissions that occurred between 2010 and 2018. Increasing energy costs and increasing environmental awareness have led people to use waste (solid, liquid, gas) from industrial factories. Significantly, many waste

heat sources (WHSs) can be obtained from the iron-steel factory working in our region [4].

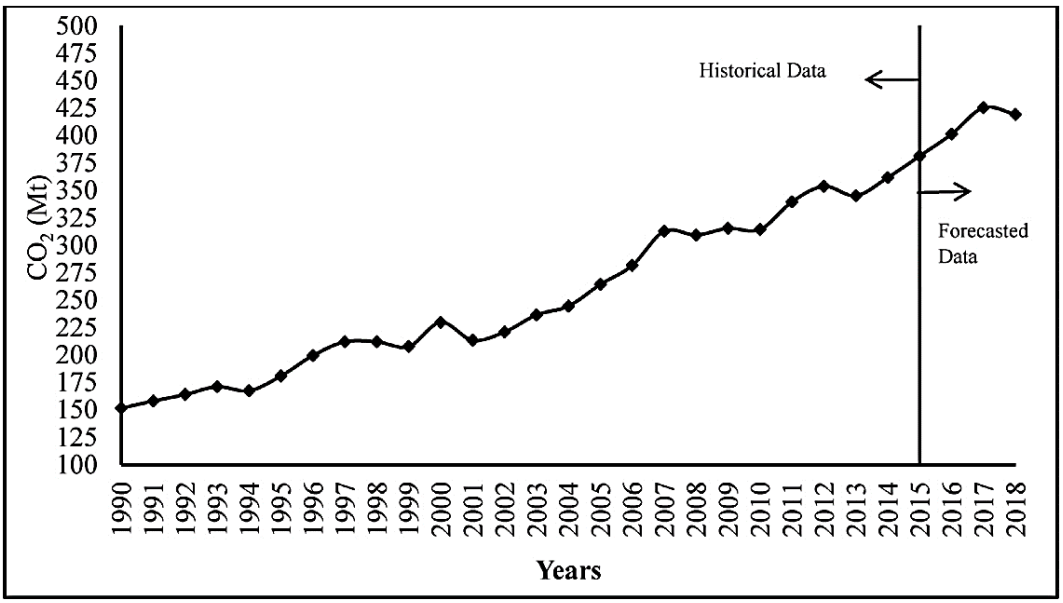

Figure 1.1. CO_2 emission variation in Turkey, 1990-2018 [6].

An essential aspect of energy management in industrial facilities is to use waste heat. The places where this heat can be used should be determined, and an economic evaluation of the systems that can be applied should be made [2]. Energy recovery using waste heat has recently become an important topic. Various energy recovery methods have been developed to generate energy from a power plant and meet the plant's power needs.

Figure 1.2 is a graph showing the amount of CO_2 emission by sectors. The industrial sector is among the industries that consume high amounts of energy. With the increase in annual energy consumption, the waste heat potential also increases.

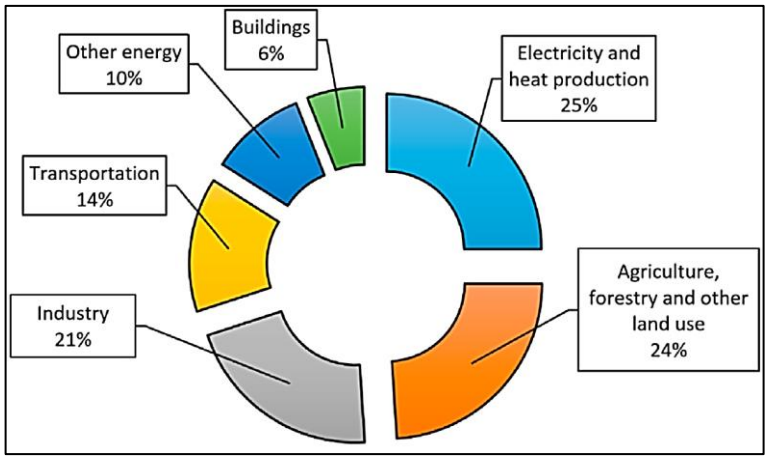

Figure 1.2. Greenhouse gas emission by sectors [6].

High-temperature (HT) flue gas is released into the atmosphere in the iron-steel facilities [7,8]. It may be possible to convert this waste heat into electrical energy using various energy conversion methods. The use of this waste heat will contribute to reducing CO_2 emissions and increasing system efficiency, as well as electricity generation. The iron-steel industry is one of the sectors that consume the most energy, with an annual energy consumption of approximately 24 EJ (24x1018 J). This consumption corresponds to 5% of the total energy consumption of the world [2].

The primary source targeted in reducing product costs is the energy costs that take the largest share with 27-33% of the production costs of the sector. Furnaces, especially annealing furnaces operating at high temperatures, are systems that should be performed as efficiently as possible in terms of fuel consumption and the pollution caused by the combustion gases discharged from the chimney in industrial enterprises [2].

The temperature of the hot exhaust gases discharged into the atmosphere depends on the process temperature and whether a WHRS is used to decrease the system's temperature. Between 93° C and 1650° C, the temperature of the gases. Three temperature regimes for the classification of WHSs are shown in Figure 1.3.

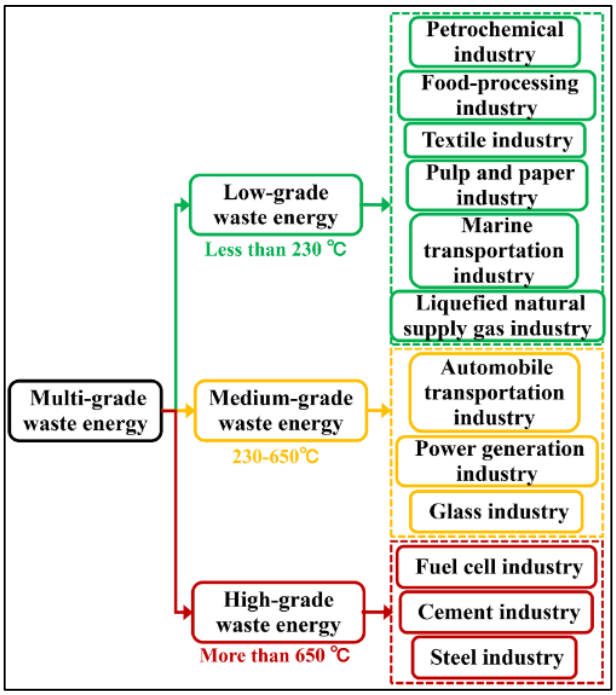

Figure 1.3. Temperature regimes for classification of industrial waste heat [9].

As shown in Figure 1.4, in the iron-steel production process, a lot of waste energy sources such as sintering ore, waste heat, flue gas, SH coke, by-product gas, smelting slag, and cooling water are generated [7,8].

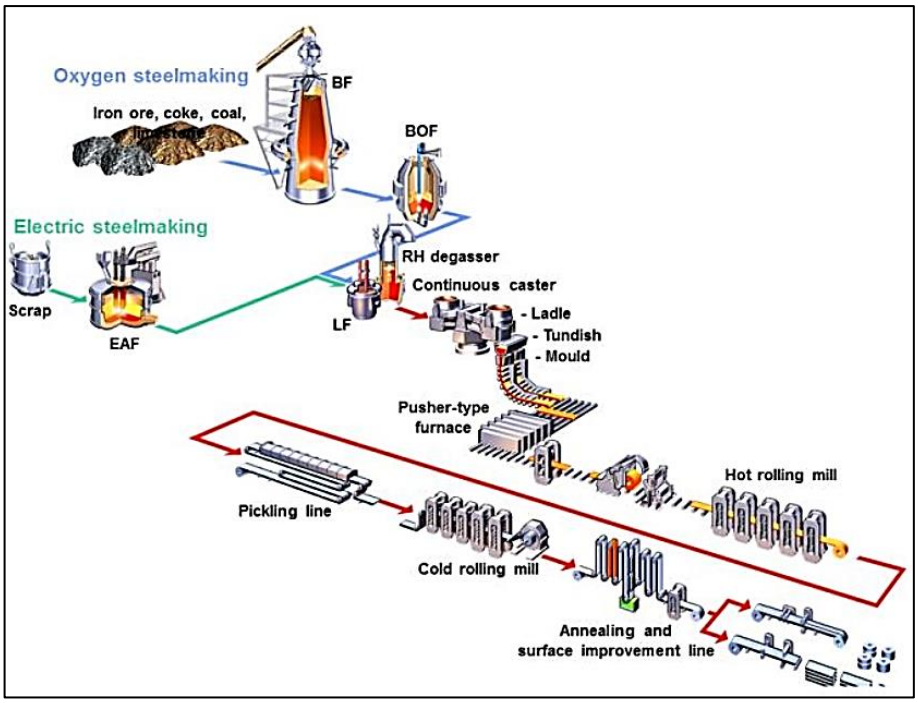

Figure 1.4. A simple scheme of iron-steel production processes [10].

Annealing furnaces represent 67% of the energy used in iron-steel facilities. The annealing furnace is used for heat treatment, especially after cold rolling, when the metallurgical structure makes the steel brittle. Utilizing combustion gases at temperatures of 800–900°C, 31.36% of the furnaces' total energy is thrown into the atmosphere. The power used to heat a portion of the processed steel is expressed as specific energy [8]. The process of an annealing furnace showed in Figure 1.5.

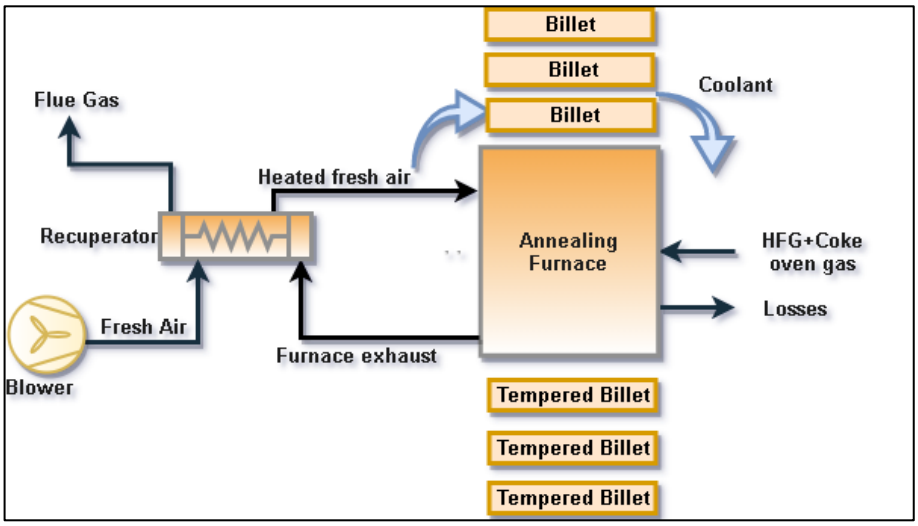

Figure 1.5. Annealing furnace process.

Many researchers studied on heat recovery from low-temperature (LT) WHSs. In this study, the use of various energy conversion methods of medium and HT waste heat and LT waste heat will increase system efficiency while helping to generate electricity.

Figure 1.6 represents the energy flow tower showing the energy quality of different WHSs and the technologies used in response to this energy. The HT heat source and Steam Rankine Cycle (*SRC*) convert some of the thermal energy to mechanical work.

SRC can be defined as a steam generator that superheats a fluid that is expanded in a turbine to generate power using waste heat.

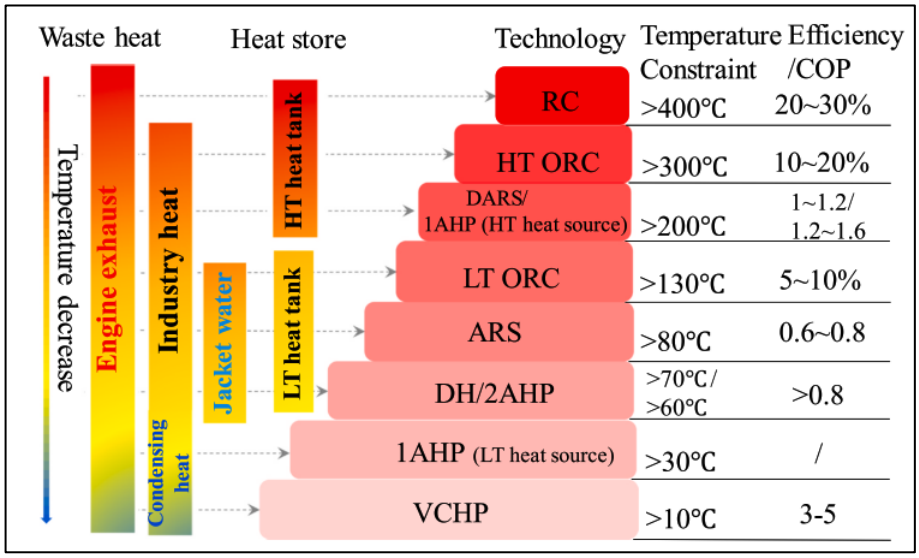

Figure 1.6. Quality of WHSs and recovery practices equivalent to this quality [9].

The Organic Rankine Cycle (*ORC*) is an effective solution for low-grade waste heat utilization. It is a closed-loop system in which the working fluid is constantly circulating through four components. If you study, the cycle system is called the *ORC* if the fluid is chosen as an organic fluid instead of water. Solar energy, geothermal energy, WHR and biomass applications can be given as a sample of *ORC* applications [11]. Since the Kalina Cycle (*KC*) patent was received in the 1980s, several studies have been studied for various power generation applications from multiple thermal sources, including energy recovery of exhaust gases.

Another thermodynamic cycle used in WHR is *KC*. The *KC* generates electricity from waste heat using a working fluid with two different boiling points. The *KC* has better achievement compared to the traditional *SRC* as the ammonia-water mixture (AWM) evaporates non-isothermally. The KC's efficiency is because the temperature is not constant during heat transfer in the evaporator and condenser. This is due to the different boiling and condensing temperatures of the working fluid used in the *KC* [12].

Different methods such as preheating, absorption cooling, thermodynamic cycles, heat pump and thermal energy storage have been developed in terms of WHR. The recovery WHR has an essential effect on increasing economic benefits and reducing the environmental pollution. Low-grade waste heat is not used efficiently in industrial processes, although heat integration has been made between process streams. It has been reported that about 50% of the total energy input is industrial waste heat from the LT range. It is possible to see many studies in the literature that provide industrial WHR using different cycles and different fluids [13].

Zhang et al. developed an original technoeconomic model for the recycling of waste energies. They set up various scenarios to assess declining energy consumption and future energy savings potential. According to their results, it has been seen that the energy-saving potential is less than 20%. The most sensitive parameters for waste energy recycling have been determined. It has been observed that approximately 44% of the waste heat can be recovered with the techno-economic model they work with. [14].

Ishaq et al. examined the performance and appropriateness of a waste heat recovery system. Hydrogen production is aimed with the thermochemical copper chlorine cycle combined with a reheated *RC* and hydrogen compression. The waste heat obtained from the slag was used as the heat source of the copper-chlorine loop. Hydrogen produced by using waste heat is evaluated in terms of first and second law efficiencies of thermodynamics. The system studied has been modeled and simulated in ASPEN Plus. The multi-generation system helps to reduce industrial waste heat usable and to operating costs significantly. As a result, the system's energy efficiency is 32.5%, while the exergy efficiency is 31.8%. [15].

Kose et al. evaluated the performance improvement of systems using *SRC* and *ORC* cycles for variable turbine inlet pressure and temperature in a *GT*-based integrated system. The *SRC* has been studied parametrically for variable temperature and pressure values, and the *ORC* has been studied parametrically for different liquids. As a result, the best working fluid was observed *R141b*. In the *ORC* system using *R141b* as the working fluid, the net power, exergy efficiency and maximum net thermal efficiency

of the system at 225 °C and 40 bar is 780.35 kW, 64.76%, and 22.6%, respectively. The efficiency and net heating value of the *GT-SRC-ORC* system with *R141b* fluid were calculated as 67.35% and 47.65%. Thus, WHR corresponding to 734.57 kg/h natural gas equivalent to 2203.73 kg-CO_2/h emission was realized [16].

Liu et. al. proposed a unique WHR system has been submitted to recycle the waste heat generated from the marine engine. In this system, *SRC* and *ORC* loops are combined to convert the marine engine's jacket cooling water and exhaust gas waste heat into mechanical energy. The proposed system is simulated and compared with the performance of WHRSs based on *SSRC* and *DPORC*. It has shown that at 100% engine load, the engine's thermal efficiency can increase by 4.42% thanks to the proposed system and can reduce fuel consumption by 9322 tons per year, while a WHRS based on *SSRC* and *DPORC* can only increase the temperature. The efficiency is 2.68% and 3.42%, respectively. [17].

Zhang et al. evaluated the performance of the *ORC*, where waste heat at a temperature of 40-140 C is used as a source, with RefProp8.0 software. *R601*, *R601a*, *R600a*, *R141b*, *R245fa* and *R245ca* working fluids have been found to have better thermal performance for lower temperature welds [18].

Song et al. using the waste heat obtained from the engine's exhaust gas and jacket cooling water designed two different *ORC* systems to select the most suitable working fluid and define the optimum system. The design and economic analysis of the designed system have been made. It has been shown that the system is technically feasible and economically attractive according to the simulation results obtained [19].

Zare et al. proposed two combined cycles, *GT-MHR/ORC* and *GT-MHR/KC*, in their studies. They aimed to make a comparison between their KC and ORC performances for WHR from *GT-MHR*. Based on the first and second laws of thermodynamics, they made a comprehensive analysis and efficiency study on this subject and worked parametrically. The performances of the loops have been optimized using EES (Engineering Equation Solver) software. According to their results, it was found that using *ORC* for *GT-MHR* WHR is more convenient than *KC*. The first and second law

yields of *GT-MHR/ORC* were higher than that of the combined *GT-MHR/KC*. And the helium mass flow rate in *GT-MHR/ORC* is significantly lower than the combined *GT-MHR/KC*. Moreover, the high-pressure level of *ORC* is much lower than that of *KC* under optimized conditions. In addition, the *ORC* prevented superheated steam droplet erosion at the turbine outlet and allowed reliable operation when the flow from the *KC* turbine was a two-phase flow [20].

Nemati et al. performed a thermodynamic optimization and modeling to compare the advantages and disadvantages of the *ORC* and the *KC* for WHR from the *CGAM* cogeneration system. They performed thermodynamic models for combined *CGAM/ORC* and *CGAM/KC* systems and investigated the effects of some decision variables on the energy and exergy efficiency and turbine size parameters of the combined systems. They have done the solution and optimization process of simulation equations with EES software by using the direct search method. It has been observed that the power generated by the cycles has minimum values at the optimum pressure ratio of the compressor. Also, optimization of the evaporator pressure performance has been done, but it has been observed that this optimum pressure level at *ORC* (11 bar) is much lower than that of *KC* (46 bar). In addition, the more straightforward configuration of the *ORC*, the superheated turbine output leading to higher net generated power and reliable performance for the turbine have been other advantages of the *ORC*. The comparison between *KC* and *ORC* concludes that *ORC* has attractive privileges for WHR in this case [21].

Singh et al. examined the possibility of being applied to electricity using LT exhaust gas heat. They combined the *KC* loop with a coal red steam plant and simulated this system. The designed model was also used to determine the optimum operating conditions for the *KC*. The effect of turbine inlet pressure and ammonia mass fraction in the mixture on the performance of the cycle was investigated. As a result, it has been seen that there is an optimum ammonia fraction value that provides maximum cycle efficiency according to a certain turbine inlet pressure. With the increase in turbine inlet pressure, the maximum loop efficiency has also increased. *KC* developed a MATLAB program for loop optimization and calculations. With a pressure of 4000 kPa and an ammonia fraction of 0.8 at the ammonia turbine inlet, the lower loop

efficiency reached a maximum of 12.95% when the exhaust gas temperature dropped from the current 407.3 K to 363.15 K. Maximum exergy degradation was found in the *KC* evaporator [22].

Ali et al. from *SOFC*, double loop *ORC* combined with a solid oxide fuel cell system connected to a gas turbine (*SOFC-GT*) for WHR and unique combined cycle configuration to exploit cold energy in liquefied natural gas (*LNG*) has been proposed. The upper *ORC* used WHR from the *SOFCGT*, while the lower *ORC* used cold energy as a heat well; They also said that the *LNG* stream can also be used for home cooling and can also generate electricity by passing it through a turbine. They used 20 different *ORC* fluids in their study. *SOFC* and *ORC* WHR system models were solved with MATLAB software with the help of the working fluid properties provided from REFPROP V9. The combination of ethane (lower loop) and R601 (upper loop) has been proposed for a double loop *ORC* system for the optimum balance between cost and efficiency. Economic analysis of the proposed *SOFC-GT-ORC* system shows that the production cost of an electric unit is $ 33.2 per MWh, which is 12.9% and 73.9% lower than the leveled electricity cost of separate *SOFC-GT* and *SOFC* systems, respectively [23].

Ozahi et al. optimization of *ORC* and performed thermodynamics and thermoeconomic analysis. The system is adapted for power generation to an existing solid waste power plant with a power capacity of 5.66 MW. They have used the actual business data of the facility in all stages of their analysis. It is aimed to convert *ORC* system at a temperature of 566 °C to electricity using an orc system. Toluene, octa metyltric hyloxane (MDM), Octametic cyclo tetras hyloxane (D4) and four different operating liquids as N-dean have taken into account the existing system and have performed analysis. As a result of thermoeconomic analyzes, toluene observed that the maximum power output of 584.6 kW is the optimum operating fluid with maximum power output and 15.69% exertion efficiency. The optimization of the loop has made the non-dominant sorting genetic algorithm method (NSGA-II) in MATLAB software environment. Optimization results compared and the total cost of cost with net power output to toluene - 5,89%, -3,51 $/h; 0.96% for MDM, -3.60 $/h; 8.45% for D4, 2.00% for -2.04 $/h and N-dean, -5.54 $/h [24], respectively.

Within the scope of the study, the mass flowrate was studied parametrically from 0.95 kg/s to 1.35 kg/s in the *SRC* cycle (using water as the working fluid). In the *ORC* cycle (using *R245fa*), the mass flow rate was studied parametrically from 2.75 kg/s to 18.5 kg/s. *KC* (using NH_3-H_2O) was investigated in terms of various turbine inlet temperatures (*TIT*) in the range of 450-490 K, and in the *SRC-ORC-KC* combined cycle, the flue gas temperature difference (ΔT) was studied parametrically between 300-430 K and *SRC-ORC-KC* combined systems were optimized.

In the iron-steel facilities, promising electricity production cost was provided by WHR systems. Power cycles are extensively studied, comparing both in terms of economy and thermal efficiency. A significant reduction was achieved in CO_2 emission production by using heat recovery systems. The net power output of the *SRC*-CO_2 combined system is 1274 kW, the thermal efficiency is 0.36, and the electricity generation cost is 0.01153 $/kWh at an optimum mass flow rate. The net power output of the *ORC*-CO_2 combined system is 766.2 kW, the thermal efficiency is 0.21, and the electricity generation cost is 0.01534 $/kWh at an optimum mass flow rate . The net power output of the *KC*-CO_2 combined system is 935.6 kW, the thermal efficiency is 0.26, and the electricity generation cost is 0.08427 $/kWh at an optimum mass flow rate. According to the optimum ΔT of the *SRC-ORC-KC* combined system, the net power output, thermal efficiency and electricity generation cost are 1010 kW, 0.44, and 0.01706 $/kWh, respectively.

SECTION 2

THEORITICAL BACKGROUND

2.1. COMBINED SYSTEMS

Waste heat recovery is based on HT exhaust gases as an input to an energy conversion system. Therefore, the degree of waste energy is significant for choosing the right energy conversion technology. In this study, an iron-steel production facility operating in the annealing furnace flue gas in Turkey will focus on assessing. In this section, four different combined systems designed for WHR from an annealing furnace were studied in detail. Four different combined cycles were used in power generation systems, respectively *SRC-CO_2*, *ORC-CO_2*, *KC-CO_2* and *SRC-ORC-KC* combined systems. The mass flow rate was studied parametrically from 0.95 kg/s to 1.35 kg/s in the *SRC*. In the *ORC*, the mass flow rate was studied parametrically from 2.75 kg/s to 18.5 kg/s. *KC* was investigated in terms of various *TIT* in the range of 450-490 K. In the SRC-ORC-KC combined system, the flue gas ΔT was investigated studied parametrically between 300-430 K.

2.1.1. *SRC-CO_2* combined system

SRC is an additional cycle that generates electrical power from the system by utilizing the waste heat of flue gas. The flue gas temperature range to be used for this system is 1093.15 K-393.15 K, that is, the temperature obtained from an industrial annealing furnace. Therefore, this system can be used in various branches of industry. Figure 2.1 shows the configuration of the *SRC-CO_2* combined system. The flue gas waste heat at 1093.15 K is used as a heat source in *SRC*, and electrical energy is produced from the steam turbine. The steam coming out of the turbine is condensed using the CO_2 cycle, and electrical work is obtained. In other words, here, the CO_2 cycle is used to generate electricity with *LT* heat recovery.

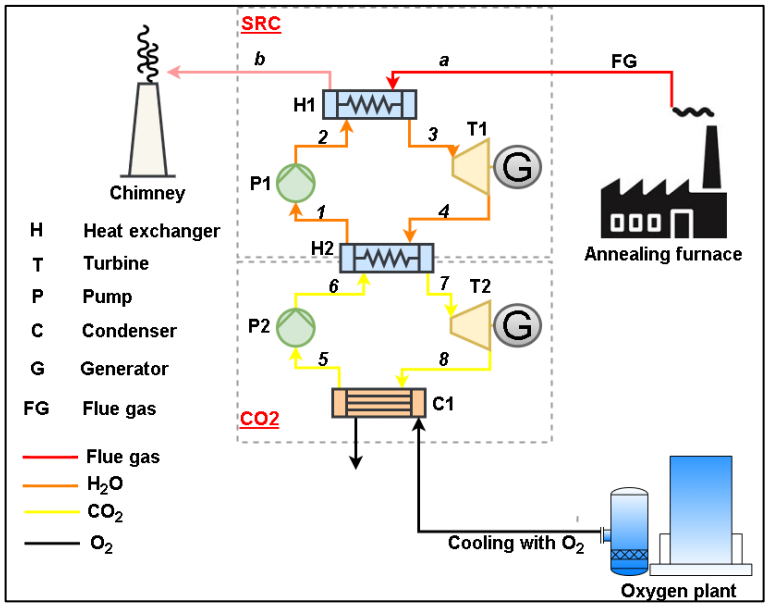

Figure 2.1. Schematic layout of the combined *SRC-CO₂* combined system.

The *SRC* consists of 4 components: Condenser, pump, heat exchanger and steam turbine, respectively. The CO_2 cycle has three components (condenser, pump and turbine) because the condenser of the SRC cycle is used as the evaporator of the CO_2 cycle. The waste heat of the annealing furnace at 1093.15 K is used as the heat source for the evaporator (from a point). The waste heat at 393.15 K from point b is released into the atmosphere. Work fluid is pressured from a 0.6 bar to 125 bar in pump (1→ 2) and sent to the evaporator to get superheated phase (2→3). The superheated steam phase is expanded to condenser pressure, and temperature in the steam turbine and mechanical work (3→4) is achieved. The steam, transferred to the condenser, is returned into a liquid phase to complete its cycle (4→ 1). The rejected heat from vapor condensation in *SRC* is employed as a heat resource for CO_2 cycle (6→7). CO2 enters the pump to be pressurized from 10 bar (5→ 6) up to condenser pressure 15 bar in the liquid phase. CO_2 in high temperature is expanded in the turbine CO_2 turbine (7→8), and mechanical work is obtained. Oxygen (O_2) is supplied in 200 K from an oxygen plant established for providing pure O_2 requirements in burning processes used in the condenser to condense the CO_2. Hence, *SRC-CO₂* combined power cycle is completed. *SRC-CO₂* combined system was parametrically optimized for mass flow (from 0.95 to 1.35 kg/s).

2.1.2. *ORC-CO₂* combined system

ORC is a power cycle that generates electricity using different organic fluids instead of water. For this system, annealing furnace flue gas in the temperature range of 1093.15-393.15 K was used as the source. In Figure 2.2, the waste heat of the flue gas is the heat source of the *ORC* cycle. The heat released from the condenser of the *ORC* cycle is the heat source of the CO_2 cycle. By the way, CO_2 provides condensation of *R245fa*. Oxygen from an oxygen plant in CO_2 condensation is integrated into the cycle.

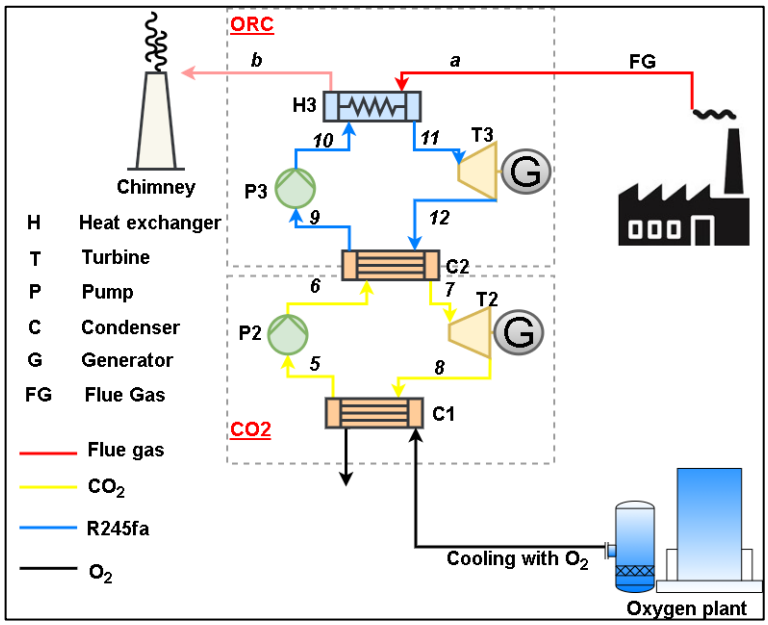

Figure 2.2. Schematic layout of the combined *ORC-CO₂* combined system.

The waste heat of the annealing furnace at 1093.15 K is used for a heat source for the evaporator (from a point). The waste heat at 393.15 K (from point b) is released into the atmosphere. *R245fa* is pressured from 1.5 bar to 20 bar in the pump (9→ 10) and sent to the evaporator to get a superheated phase (10→11). The superheated steam phase is expanded to condenser pressure, and temperature in the *ORC* turbine and mechanical work (11→12) is achieved. The steam, transferred to the condenser, is returned into a liquid phase to complete its cycle (12→9). The rejected heat from vapor condensation in *SRC* is employed as a heat resource for CO_2 cycle (6→7). CO_2 enters the pump to be pressurized from 10 bar (5→ 6) up to condenser pressure 15 bar in the liquid phase. CO_2 in high temperature is expanded in the turbine CO_2 turbine (7→8),

and mechanical work is obtained. O_2 is supplied in 200 K from an oxygen plant established for providing pure O_2 requirements in burning processes used in the condenser to condense the CO_2. Hence, *ORC*-CO_2 combined cycle is completed. *ORC*-CO_2 combined system is parametrically optimized for mass flow (from 2.75 to 18 kg/s).

2.1.3. *KC*-CO_2 combined system

The *KC*, a variant of the *SRC*, uses ammonia water as the working fluid. The temperature profile during condensation and boiling is the essential difference between systems using one fluid and two fluids. Examples of a single fluid cycle are *SRC* and *ORC*. In single fluid cycles, the temperature remains constant during boiling and condensation. As heat is transferred to the working fluid (e.g., water), the fluid's temperature gradually comes to boiling point and then remains constant until the liquid evaporates. In the *AWM* with different boiling point temperatures used in a second fluid cycle, temperature increase occurs during evaporation, while temperature decrease occurs during condensation. In Figure 2.3, the waste heat of the flue gas is the heat source of the *KC*.

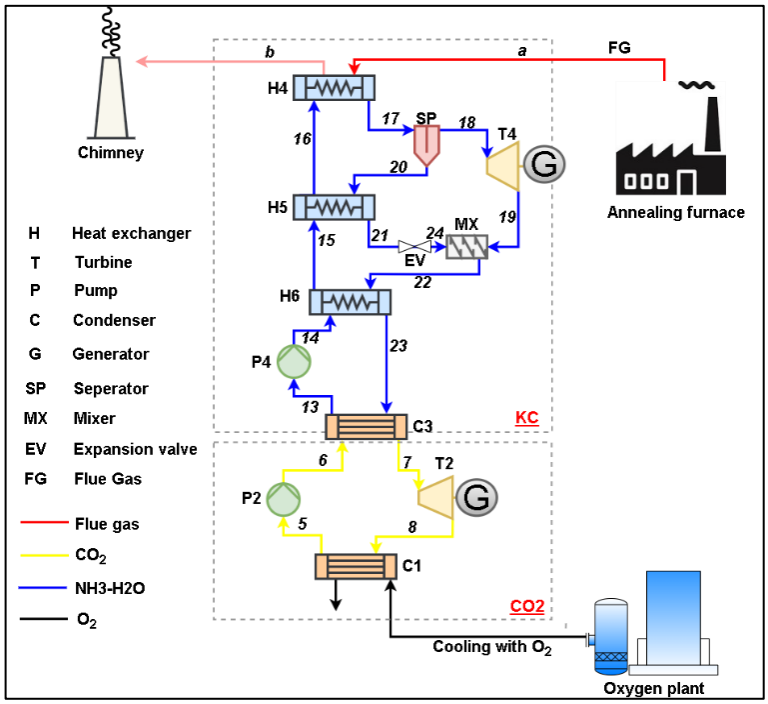

Figure 2.3. Schematic layout of the combined *KC*-CO_2 combined system.

The waste heat of the annealing furnace at 1093.15 K is used as the heat source for KC (from a point). The waste heat at 393.15 K (from point b) is released into the atmosphere. The *AWM* (0.65 ammonia + 0.35 water) is pressurized (13→ 14) from 10 bar to 60 bar in pump and sent to the low-temperature recuperator (*LTR*) (14→ 15) and high-temperature recuperator (*HTR*) (15→ 16), respectively, to preheat the AWM mixture gradually. In the separator, rich ammonia vapor is separated (17→ 18) and sent to the turbine for generating mechanical work (18→ 19). The liquid phase AWM from the separator is transferred to the *HTR* (20→ 21), and the expansion valve reduces pressure (21→ 24) to condenser pressure. Rich ammonia water leaving from turbine and weak *AWM* from expansion valve mixed in the mixer (19,24→ 22). The mixture flows to *LTR* before the condenser (22→ 23). The rejected heat from condensation of the *AWM* in *KC* is employed as a heat resource for CO_2 cycle (6→7). CO_2 enters the pump to be pressurized from 10 bar (5→ 6) up to condenser pressure 15 bar in the liquid phase. CO_2 in high temperature is expanded in the turbine CO_2 turbine (7→8), and mechanical work is obtained. O_2 is supplied in 200 K from an oxygen plant established for providing pure O_2 requirements in burning processes used in the condenser to condense the CO_2. Hence *ORC*-CO_2 combined cycle is completed. *KC*-CO_2 combined cycle is parametrically optimized for mass flow (from 1 to 10 kg/s).

2.1.4. *SRC-ORC-KC* combined system

The waste heat leaving the burning process at 1093.15 K is first used (point a) as the heat source of the *SRC*. The flue gas leaving the *SRC* evaporator with 693.15 K used (point b) as the heat source of the *ORC*. The flue gas leaving the *ORC* evaporator with 493.15 K was used (point c) as the heat source of the *KC*, and the flue gas was rejected from the system with 393.15 K (point d). In Figure 2.4 depicts *SRC-ORC-KC* combined system.

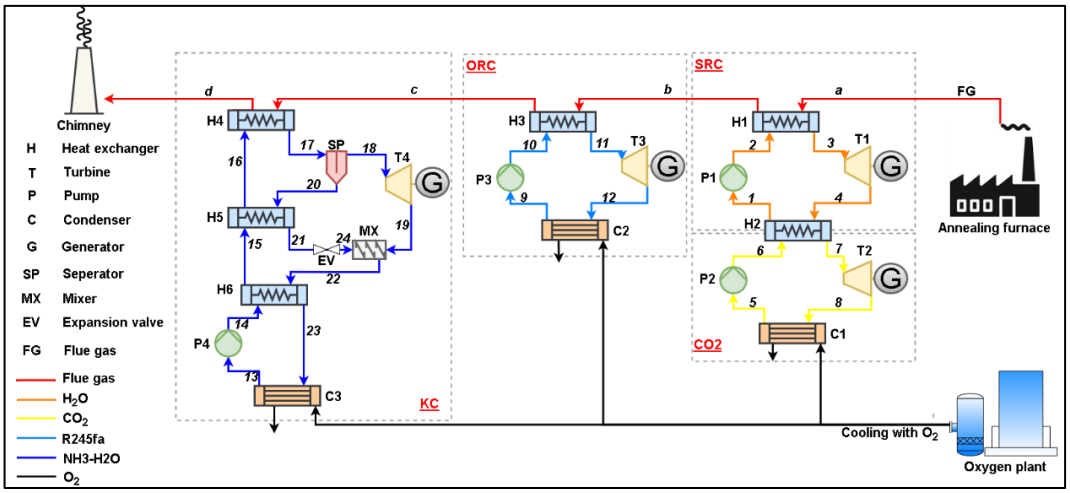

Figure 2.4. Schematic layout of the *SRC-ORC-KC* combined system.

The volumetric percentages of the flue gas components were measured using a flue gas analyzer. The density and specific heat of the flue gas were calculated using EES depending on the average flue gas temperature. Table 2.1 represents thermophysical properties of the existing flue gas supplied from the annealing furnace.

Table 2.1. Thermophysical properties of the existing flue gas supplied from the annealing furnace.

Parameter	Value	Unit
$T_{out,fg}$	1093.15	K
V_{fg}	40000	m^3/h
ρ_{fg}	0.3027	kg/m^3
$C_{p,fg}$	1.382	kJ/kgK
P_{fg}	101.325	kPa

Several combined cycles are designed and analyzed to recover the exhaust gas from the annealing furnace. In this way, it is aimed to increase the overall system efficiency. The thermophysical properties of the existing flue gas obtained from the annealing furnace are given in Table 1. Mass flow rate has been studied parametrically for *SRC-CO_2* and *ORC-CO_2* combined cycles. In parametric study *TIT* is calculated depending on the mass flow rate of *SRC*. Similarly, with the change of mass flow rate, the amount of heat to be discharged from the *SRC* cycle to the *CO_2* cycle will also vary. The power

cycle to be obtained when using only *SRC-CO_2* in the flue gas, the power cycle to be obtained when only *ORC-CO_2* is used, the power to be accepted when only *KC-CO_2* is used, and the overall combined system in which all cycles are combined are compared with each other. During the analysis, some design parameters for all cycles were considered constant to compare the results obtained from the cycles. The nominal parameters accepted for the *SRC* loops are given in Table 2.2. Turbine efficiency was calculated using *EES*.

Table 2.2. The accepted nominal parameters for the *SRC* [16,25].

Parameter	Value
$\eta_{s,p}$	1
η_t	0.73
ε_{hex}	0.8

Table 2.3. Several input parameters are used to model a *CO_2* cycle [26,27].

Parameter	Value
T_{CW}; in[K]	243.15
$\eta_{t,co2}$	1
$\eta_{p,co2}$	1
ε_{hex}	0.8

Table 2.4 represents several input parameters used to model *ORC*. According to the literature review, *R245fa* was chosen as the working fluid in the *ORC*.

Table 2.4. Several input parameters are used to model *ORC* [28].

Parameter	Value
T_{CW}; in[*K*]	243.15
$\eta_{t,ORC}$	1
$\eta_{p,ORC}$	1
ε_{hex}	0.8

Table 2.5 represents several input parameters used to model *KC*. The working fluid of the *KC* is a mixture. Therefore, the operating temperature and pressure range are minimal.

Table 2.5. Several input parameters are used to model *KC* [20].

Parameter	Value
T_{CW}; in [*K*]	243.15
ε_{hex}	0.8
$\eta_{t,KC}$	1
$\eta_{p,KC}$	1
x	0.65

SECTION 3

THERMODYNAMIC ANALYSIS

Analysis of each cycle is made using thermodynamic and thermoeconomic tools. The modeling of each combined cycle is done using *EES* [5]. The annealing furnace is currently operating in an iron-steel production facility. Thermophysical properties of annealing furnace flue gas were taken from the facility.

3.1. GENERAL ENERGY, MASS EQUATIONS

The energy balance equation is calculated by [16]:

$$\dot{Q} + \dot{W} = \sum m_{out} \cdot h_{out} - \sum m_{in} \cdot h_{in} \quad (3.1)$$

The mass balance equation is calculated by [16]:

$$\sum \dot{m}_{in} = \sum \dot{m}_{out} \quad (3.2)$$

$\dot{W}$ and $\dot{Q}$ refers to the work flow and the heat, respectively.

$$W_{net;\mathrm{SRC}} = W_t - W_p \quad (3.3)$$

where the W_{net} represents each cycle net power, and W_t represents the turbine power, W_p represents the pump power consumption [29].

The thermal efficiency of combined cycle is obtained by [30]:

$$\eta = \frac{W_{net}}{Q_{in}} \quad (3.4)$$

3.2. THE ENERGY EQUATION FOR *SRC*

In terms of energy, performance analysis of the *SRC* is done for the entire cycle. The overall heat transferred from the flue gas to the working fluid is achieved as follows [31]:

$$Q_{in,SRC} = m_{fg}(h_a - h_b)\,\mathcal{E}_{hex} = m_{SRC}(h_3 - h_2) \tag{3.5}$$

where m_{fg} is the mass flow rate of the flue gas in the combined cycle and m_{SRC} is the mass flow rate in the *SRC*. The net power output produced from the *SRC* is achieved as follows [32]:

$$W_{net;SRC} = W_{t;SRC} - W_{p;SRC} \tag{3.6}$$

where $W_{t;SRC}$ depicts the power generated from the *SRC* and $W_{p;SRC}$ is the power used by the *SRC* pump. The *SRCs'* thermal efficiency is calculated by [33]:

$$\eta_{\text{th}} = \frac{W_{net;SRC}}{Q_{SRC}} \tag{3.7}$$

Turbine efficiency of *SRC* is calculated by [34]:

$$\eta_{\text{t}} = \frac{h_3 - h_{4a}}{h_3 - h_{4s}} \tag{3.8}$$

3.3. THE ENERGY EQUATION FOR CO_2

The total heat transferred from condenser of *SRC* to CO_2 cycle working fluid is obtained by [35,36]:

$$Q_{CO2} = m_{SRC}(h_4 - h_1)\mathcal{E}_{hex} = m_{CO2}(h_7 - h_6) \tag{3.9}$$

where m_{CO2} is the mass flow rate of the working fluid in the CO_2 cycle, and $\mathcal{E}_{hex}$ is the effectiveness of the heat exchanger. The net power output produced from the CO_2 cycle is calculated by [35]:

$$W_{net;CO2} = W_{t;CO2} - W_{p;CO2} \tag{3.10}$$

where $W_{t;\,CO2}$ represents the power generated from the CO_2 turbine and $W_{p;CO2}$ is the power used by the CO_2 pump. The thermal efficiency of the CO_2 cycle is calculated by [37]:

$$\eta = \frac{W_{net;CO2}}{Q_{CO2}} \tag{3.11}$$

3.4. THE ENERGY EQUATION FOR *ORC*

The overall heat, received from flue gas to the *R245fa* is obtained by [38]:

$$Q_{ORC} = m_{fg}(h_b - h_c)\mathcal{E}_{hex} = m_{ORC}(h_{11} - h_{10}) \tag{3.12}$$

where m_{ORC} is the mass flow rate of the *R245fa* in the *ORC* and $\mathcal{E}_{hex}$ is the effectiveness of the heat exchanger. The net power output from the *ORC* is calculated by [28]:

$$W_{net;ORC} = W_{t;ORC} - W_{p;ORC} \tag{3.13}$$

where $W_{t;ORC}$ shows the power from the *ORC* turbine and $W_{p;ORC}$ is the power used by the *ORC* pump. The thermal efficiency of the *ORC* is calculated by [11]:

$$\eta = \frac{W_{net;ORC}}{Q_{ORC}} \tag{3.14}$$

3.5. THE ENERGY EQUATION FOR *KC*

The overall heat, received from flue gas to the *AWM* is obtained by [39]:

$$Q_{KC} = m_{fg}(h_c - h_b)\mathcal{E}_{hex} = m_{KC}(h_{17} - h_{16}) \quad (3.15)$$

where m_{KC} is the mass flow rate of the *AWM* working fluid in the *KC* and $\mathcal{E}_{hex}$ is the effectiveness of the heat exchanger. The net power output produced from the *KC* is calculated by [20]:

$$W_{net;KC} = W_{t;KC} - W_{p;KC} \quad (3.16)$$

$W_{t;KC}$ represents the power generated from the *KC* turbine, and $W_{p;KC}$ is the *KC* pump's power. The thermal efficiency of the *KC* is calculated by [40]:

$$\eta_{KC} = \frac{W_{net;KC}}{Q_{KC}} \quad (3.17)$$

The thermal efficiency of the *SRC-ORC-KC* combined system can be written as [20]:

$$\eta = \frac{(W_{net;KC} + W_{net;CO2} + W_{net;SRC} + W_{net;ORC})}{Q_{TOTAL}} \quad (3.18)$$

In the thermodynamics analysis, the assumption of negligible kinetic and potential energies is considered under steady-state conditions. The environmental temperature is assumed as 18 °C [16].

SECTION 4

THERMOECONOMIC ANALYSIS AND ENVIRONMENTAL IMPACT

4.1. THERMOECONOMIC ANALYSIS

The system investment cost is an essential for the preliminary design of the thermal systems [36]. Thermoeconomic analysis is done to compare cycles under optimum thermodynamic conditions [41]. In this study, a thermodynamic model is designed using the *EES* program. Details on thermoeconomic analysis in the combined cycle can also be seen in the literature.

Since each device in a system is expected to operate in a certain period, the capital cost rate in *$/s* is represented by $\dot{Z}$ as [24]:

$$\dot{Z} = \frac{PEC \phi CRF}{3600N} \tag{4.1}$$

where *PEC*, *CRF*, ϕ and *N* represents the purchased equipment cost, the capital recovery factor, the maintenance factor and the annual operation time, respectively.

The maintenance factor is accepted as 1.12 and capital recovery factor is calculated by [42]:

$$CRF = \frac{i(1+i)^n}{(1+i)^n - 1} \tag{4.2}$$

In the present study, the interest rate (*i*) and the system life (*n*) are assumed to be 10% and 30 years, respectively.

4.1.1. Equipment investment cost calculation for components of *SRC*

Equipment investment cost function for evaporator of the *SRC* cycle is calculated by [43]:

$$PEC_{eva,SRC}=6570\left(\frac{Q}{\Delta \mathrm{Tm}}\right)^{0.8}+21276\dot{\mathrm{m}}_{\mathrm{rc}}+1184.4\dot{\mathrm{m}}_{\mathrm{fg}} \quad (4.3)$$

where Q, ΔTm, $\dot{\mathrm{m}}_{src}$, $\dot{\mathrm{m}}_{\mathrm{fg}}$ respectively; the heat transferred from flue gas to the *SRC* cycle, the logarithmic mean temperature difference, *SRC* cycle mass flow rate, mass flow rate of flue gas.

Equipment investment cost function for the steam turbine of the *SRC* cycle is calculated by [44]:

$$PEC_{ST}=4405\dot{\mathrm{W}}_{ST}{}^{0.7} \quad (4.4)$$

where $\dot{\mathrm{W}}_{ST}$ is the power obtained from the steam turbine.

Equipment investment cost function for the pump of the *SRC* cycle is calculated by [43]:

$$PEC_{pump,SRC}=1120\dot{\mathrm{W}}_{P}{}^{0.8} \quad (4.5)$$

where $\dot{\mathrm{W}}_{p}$ is the power consumed by the pump.

Equipment investment cost function for the condenser of the *SRC* cycle is calculated by [43]:

$$PEC_{cond,SRC}=588A_{Cond}{}^{0.8} \quad (4.6)$$

4.1.2. Equipment investment cost calculation for components of *ORC*

Equipment purchased cost function for evaporator of the *ORC* cycle is calculated by [23]:

$$PEC_{eva,ORC}=309.14A_{eva}{}^{0.85} \quad (4.7)$$

Considering the logarithmic mean temperature difference (ΔT_m) and the overall heat transfer coefficient (U) the heat transfer equation can be expressed as:

$$Q = UA\Delta T_m \quad (4.8)$$

The purchased equipment cost for the turbine of the *ORC* cycle is calculated by [23]:

$$PEC_{turbine,ORC}=4750\dot{W}_t{}^{0.75} \quad (4.9)$$

where $\dot{W}_t$ is the power obtained from the *ORC* turbine.

Equipment purchased cost function for the pump of the *ORC* cycle is calculated by [23]:

$$PEC_{pump,ORC}=200\dot{W}_p{}^{0.65} \quad (4.10)$$

where $\dot{W}_p$ is the power consumed by the pump.

Equipment purchased cost function for the condenser of the *ORC* cycle is calculated by [23]:

$$PEC_{cond,ORC}=516.62A_{cond}{}^{0.6} \quad (4.11)$$

4.1.3. Equipment investment cost calculation for components of CO_2

Equipment investment cost function for the pump of the CO_2 cycle is calculated by [36]:

$$PEC_{pump,CO2}=1120\dot{W}_P^{\,0.8} \quad (4.12)$$

where $\dot{W}_p$ is the power consumed by the pump.

Equipment investment cost function for the turbine of the CO_2 cycle is calculated by [36]:

$$PEC_{turbine,CO2}=866.64\dot{W}_T^{\,0.82} \quad (4.13)$$

where $\dot{W}_T$ is the power obtained from the turbine.

Equipment investment cost function for the condenser of the CO_2 cycle is calculated by [36,45]:

$$PEC_{Cond,CO2}=2143A_{Cond}^{\,0.514} \quad (4.14)$$

4.1.4. Equipment investment cost calculation for components of *KC*

Equipment investment cost function for evaporator of the *KC* cycle is calculated by [46]:

$$PEC_{eva}=130\left(\frac{A_{\mathrm{eva}}}{0.093}\right)^{0.78} \quad (4.15)$$

Equipment investment cost function for separator of the *KC* cycle is calculated by [46]:

$$PEC_S=114.5\dot{m}_{17}^{\,0.67} \quad (4.16)$$

where $\dot{m}_{17}$ is the mass flow rate before the separator. Equipment investment cost function for the turbine of the *KC* cycle is calculated by [47,48]

$$PEC_{turbine}=4405\dot{W}_T^{0.7} \quad (4.17)$$

Equipment investment cost function for the mixer of the *KC* cycle is calculated by [46]:

$$PEC_{mx}=114.5\dot{m}_{20}^{0.67} \quad (4.18)$$

Equipment investment cost function for the condenser of the *KC* cycle is calculated by [44,46]:

$$PEC_{cond}=130\left(\frac{A_{\mathrm{Cond}}}{0.093}\right)^{0.78} \quad (4.19)$$

The investment cost function for the *HTR* of the *KC* cycle is calculated by [46,47]:

$$PEC_{HTR}=2681\left(\frac{A_{\mathrm{HTR}}}{0.098}\right)^{0.59} \quad (4.20)$$

The investment cost function for the *LTR* of the *KC* cycle is calculated by [46,47]:

$$PEC_{LTR}=2681\left(\frac{A_{\mathrm{LTR}}}{0.098}\right)^{0.59} \quad (4.21)$$

Equipment investment cost function for expansion valve of the *KC* cycle is calculated by [46]:

$$PEC_{exp}=114.5\dot{m}_{20} \quad (4.22)$$

4.2. ENVIRONMENTAL IMPACT

The effect of the emission of air pollutants must be taken into account to protect the environment. Environmental analysis is an important parameter to measure the amount of emissions released in the atmosphere and save environmental costs by reducing emissions [49,50]. The specific CO_2 emission factors are gathered from [51]

Considering the CO_2 emission, various fuels have specific CO_2 emission amounts. When fuel is used for electricity generation, the amount of CO_2 emission increases with the system's efficiency. For instance, if electricity from a *SRC* with 30% efficiency had been obtained from a power plant using coal, 4159 tons of CO_2 emissions would be released into the atmosphere. If the electricity we produced with the amount of heat transfer we obtained from the flue gas we used in our study had been obtained from a power plant using natural gas, 2198 tons of CO_2 would have been emitted.

Therefore, by providing the transfer of the flue gas with the recuperator to various combined cycles, we also prevent the high amount of CO_2 emission released into the atmosphere and contribute to protecting the climate in the short term.

SECTION 5

SIMULATION OF WASTE HEAT RECOVERY WITH COMBINED CYCLES BY EES

5.1. EES

EES is an equation-solving program that can solve many non-linear algebraic and differential equations. The program offers integral solutions, optimization, uncertainty analysis, linear or non-linear regression, unit conversion and graphing.

The most crucial feature of *EES* is the highly accurate thermodynamic and transport featured database that allows it to be used with equation solving features for hundreds of substances.

5.1.1. Basis Feature

- In any order, the equation can be entered.
- Breakneck calculation speed
- Univariate and multivariate optimization capability
- Link to Fortran, C/C++, Python, Excel, and MATLAB
- Professional plotting (2-D, contour, and 3-D) with automatic updating

Since *EES* prepares its database by classifying fluids, its thermodynamic calculations are highly accurate i.e.:

- Real fluids
- Air-H_2O
- Brine
- Ideal gases

- Incompressible
- Mixtures

EES needs two independent properties to calculate the thermophysical property of pure fluid. Eight thermodynamic properties are considered by the *AWM*, which is part of the proposed integrated system. These are respectively: mixture temperature, mixture pressure, ammonia mass fraction, specific enthalpy of the mixture, particular mixture entropy, the specific internal energy of mixture, certain mixture volume, vapor mass fraction.

5.1.2. Application of EES

The database properties tables make this software capable. The program user defines the inputs, then the dependent variables are calculated by *EES*. According to the given inputs, the results can be plotted, and a complex problem can be concluded quickly. For Solve fundamental problems of thermodynamics, heat transfer and fluid mechanics, *EES* is helpful software. The software is helpful for most engineering purposes. *EES* is a valuable program for solving problems in the engineering field. In this study, the *EES* program was used to model and analyze the integrated systems proposed for evaluating the annealing furnace flue gas waste heat [52].

SECTION 6

RESULTS AND DISCUSSION

The waste heat of the industrial annealing furnace was used in four different combined systems, and the results of net power output ($\dot{W}_{net}$), thermal efficiency (η_{th}), purchased equipment costs (*PEC*), electricity generation costs ($\dot{Z}_{electricity}$) were analyzed. Necessary calculations were made using the annealing furnace flue gas measurement data, energy balances were established, and heat recovery potentials were revealed. Below, the results calculated for each combined systems and the results obtained with parametric studies will be given section by section.

6.1. *SRC-CO₂* COMBINED SYSTEM

Considering the parameters calculated by the first law of thermodynamics and the second law of thermodynamics is the best way to observe the performance of a system. This way helps to give very specific information about the current state of the system. Therefore, thermal analysis is of enormous importance to make a definite decision about the system's behavior according to the operating pressure, operating temperature, and mass flow.

In this section, the parametric optimization of *SRC*, namely the net power output obtained according to the varying mass flow rate (from 0.95 kg/s to 1.35 kg/s, the combined system thermal efficiency, and the electricity generation costs are shown.

TIT and pressure of *SRC* are determined according to the literature[25]. While the *TIT* is 823 K and its pressure is 125 bar, the mass flow rate of the *SRC* is calculated as 1.141 kg/s. The *SRC* net power output obtained with this mass flow rate was calculated as 923 kW. The *TIT* and pressure of the working fluid used in the *SRC* are 319.15 K and 0.6 bar, respectively. The enthalpy at the boiler inlet was calculated by the sum of

the pump work and the condenser outlet enthalpy. According to these conditions, the temperature at the boiler entry point was calculated. The quality of the fluid entering the boiler is entirely steam, so x = 0. In the evaporator *SRC*, there is heat intake at constant pressure. *TIT* was determined according to the values used in the literature. According to these input data, thermodynamic parameters (*enthalpy*, *entropy* and *specific volume*) were calculated using *EES*. The turbine power output and efficiency obtained from a *SRC* operating under these conditions are 923 kW and 0.26, respectively. The equipment purchase cost of each component in the *SRC* has been calculated. The unit cost of electricity obtained from the *SRC* is 0.01258 $/kWh.

The heat released from the condenser part of the *SRC* is transferred to the CO_2 cycle. In the combined system, the condenser outlet pressure of CO_2 is 10 bar, and the dryness amount is x = 0. CO_2 cycle pressure value was determined according to the values obtained from the literature review. According to these data, the necessary thermodynamic parameters at the 5th point were calculated. As in the *SRC*, the pump outlet enthalpy was calculated according to the pump work and condenser outlet enthalpy in the CO_2 cycle. The CO_2 cycle *TIT* was determined according to the literature, and the turbine output power was calculated with the input parameters. The net output power of the combined system is 1041 kW.

Mass flow rate has an essential effect on transferring heat taken from the flue gas to the *SRC*.

Figure 6.1 demonstrating the $\dot{Z}_{electricity,total}$ of *SRC*-CO_2 combined system due to the change in mass flow rate. At the 5th point, where the mass flow rate is 1.034 kg/s, the minimum electricity generation cost (0.01153 $/kWh) is obtained. As a result, for the minimum $\dot{Z}$, optimum values for *TIT*, $\dot{W}_{net,total}$ and $\eta_{th,cc}$ are determined as 949.8 K, 1274 kW and 0.36, respectively.

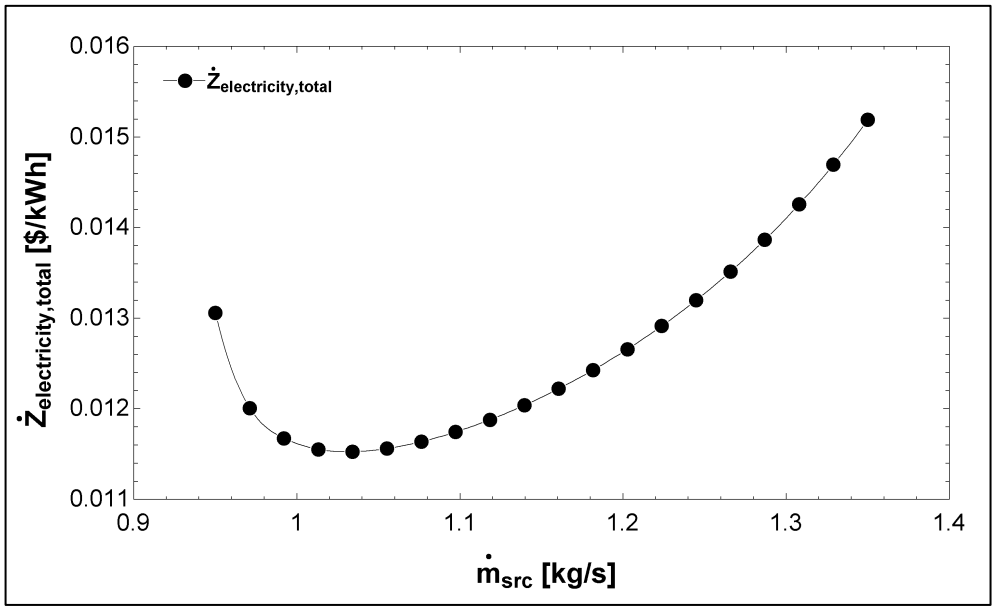

Figure 6.1. Variation of $\dot{Z}$ versus $\dot{m}_{src}$

According to Figure 6.2, *TIT* of *SRC* decreased versus increasing mass flow rate from 1072 K to 661.3 K.

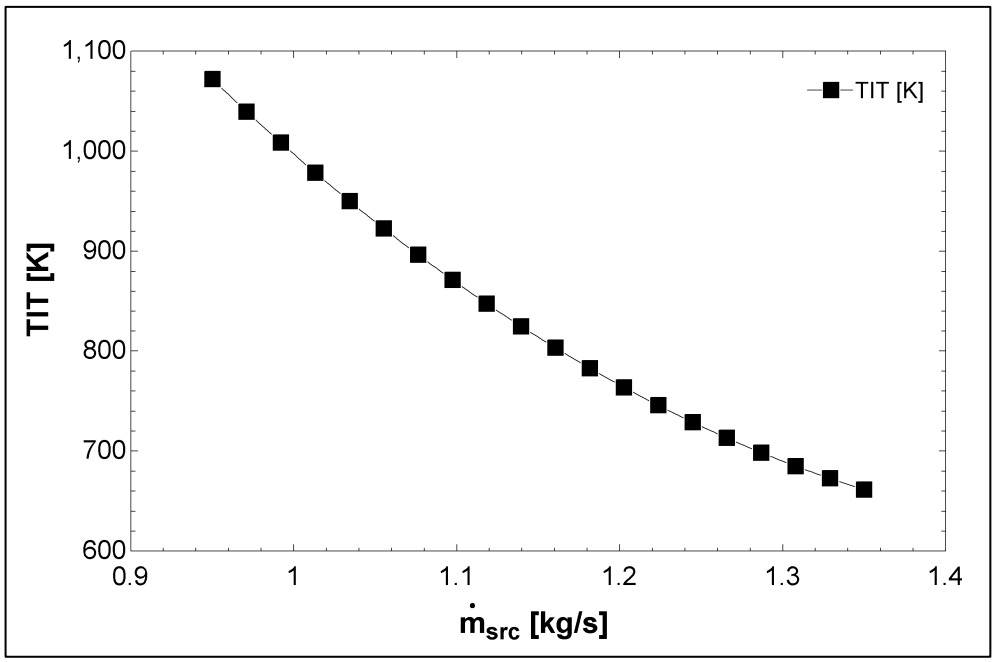

Figure 6.2. Effects of increasing mass flow rate on *TIT* of *SRC*.

Figure 6.3 represents thermal efficiency of combined system and net power output values according to the mass flow rates between 0.95 kg/s and 1.35 kg/s. The net power

output of *SRC* decreased from 1361 kW to 444.6 kW according to the increasing mass flow rate. On the contrary, the net power output of CO_2 cycle increased from 97.82 kW to 139 kW. The higher net power output *SRC* than the CO_2 cycle total thermal efficiency and net power output decreased from 0.41 and 1459 kW to 0.16 and 583.6 kW, respectively.

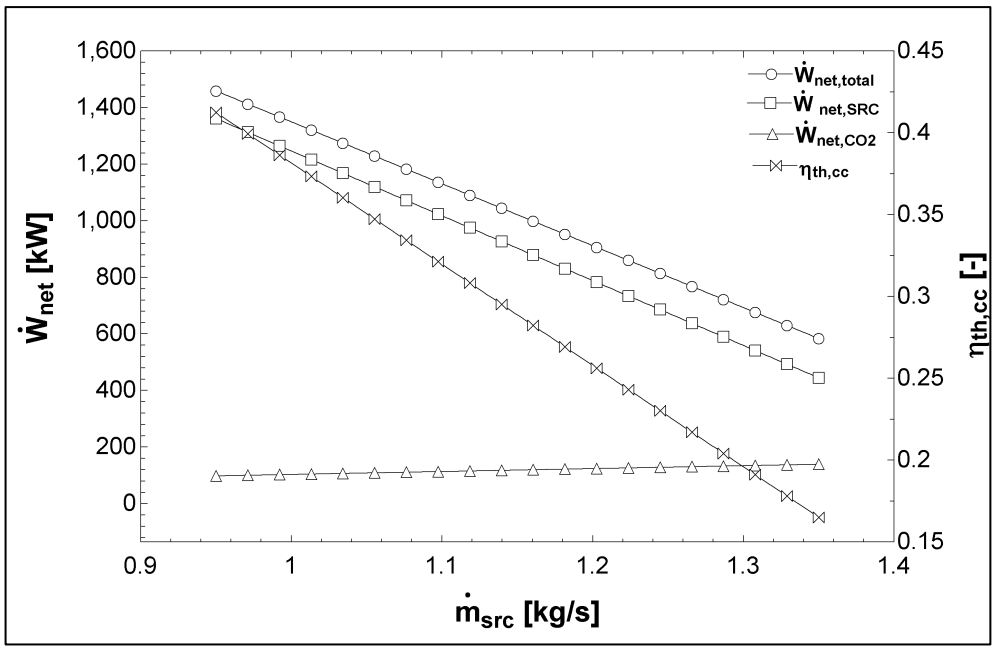

Figure 6.3. Variation of $\dot{W}_{net,total}$, $\dot{W}_{net,SRC}$, $\dot{W}_{net,CO2}$, $\eta_{th,cc}$.

To determine the minimum electricity generation cost, the parametrically studied mass flow values versus the thermal efficiency, net power output and *TIT* shown as a summary Table 6.1. Figure 6.4 represents the T-s diagram of *SRC* according to the optimum mass flow rate.

Table 6.1.Parametric results of *SRC-CO_2* combined system according to mass flow rate of *SRC*.

$\dot{m}_{src}$ (kg/s)	η_{cc} (-)	$\dot{Z}_{electricity,total}$ ($/kWh)	$W_{net,total}$ (kW)	TIT_{src}(K)
0.95	0.4124	0.01306	1,459	1,072
0.9711	0.3994	0.01201	1,413	1,039
0.9921	0.3864	0.01168	1,367	1,008
1.013	0.3734	0.01155	1,321	978.4
1.034	0.3603	0.01153	1,274	949.8
1.055	0.3473	0.01156	1,228	922.4
1.076	0.3343	0.01164	1,182	896.2
1.097	0.3213	0.01175	1,136	871.2
1.118	0.3082	0.01188	1,090	847.4
1.139	0.2952	0.01204	1,044	824.7
1.161	0.2822	0.01222	998.1	803.2
1.182	0.2692	0.01243	952.1	782.9
1.203	0.2562	0.01266	906	763.7
1.224	0.2431	0.01292	860	745.7
1.245	0.2301	0.0132	813.9	728.8
1.266	0.2171	0.01352	767.9	713.1
1.287	0.2041	0.01387	721.8	698.5
1.308	0.1911	0.01426	675.8	685
1.329	0.178	0.0147	629.7	672.6
1.35	0.165	0.01519	583.6	661.3

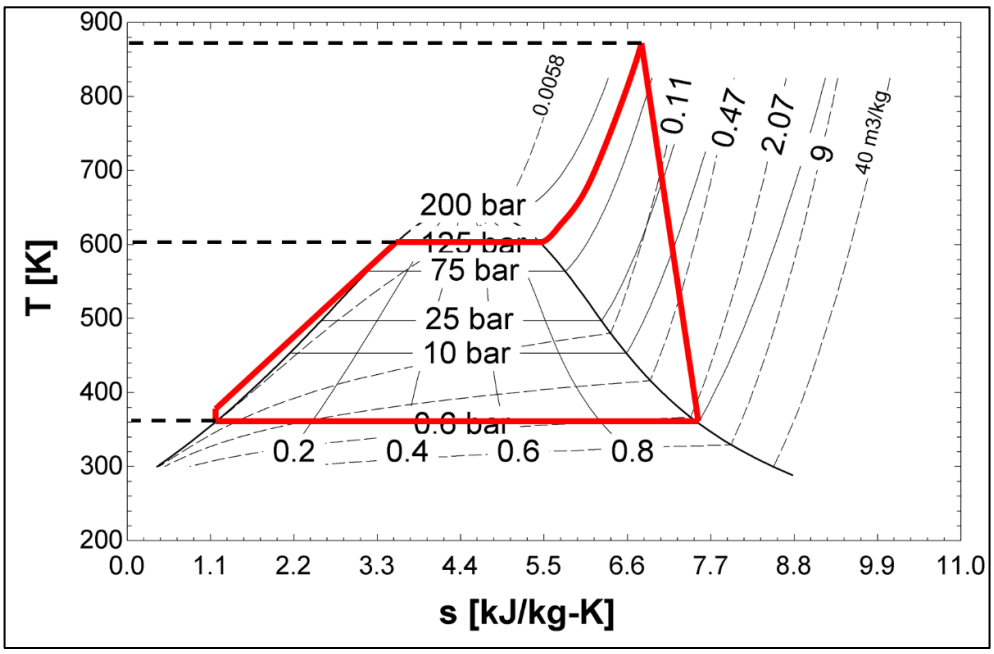

Figure 6.4. T-s diagram of *SRC*.

6.2. *ORC-CO_2* COMBINED SYSTEM

The flue gas waste heat provides power generation by transferring its heat to *R245fa*, the *ORC* working fluid in a evaporator. The heat discharged from the condenser part of the *ORC* is also taken by the CO_2 cycle, and power generation occurs. *R245fa* condenser outlet pressure 1.5 bar and temperature 298.55 K are the values determined due to the literature review. And at this point, the phase of the fluid is entirely liquid so x = 0. The thermodynamic properties of the loop at the condenser outlet were calculated according to these input parameters. Pressure and enthalpy are known for pump output data. The enthalpy is the sum of the pump work and the enthalpy at the condenser outlet, as in the *SRC*. The *TIT* was determined as 435 K as a result of literature research. Since there is a constant pressure heat transfer in the evaporator, the pump outlet pressure and the turbine inlet pressure are equal. The dryness of the fluid at the turbine outlet is x = 1. The heat transfer formula calculated the mass flow rate of the cycle. The net power output obtained from the *ORC* is 652.3 kW.

The heat released from the condenser of the *ORC* is transferred to the CO_2 cycle. In the combined system, the condenser outlet pressure of CO_2 is 10 bar, and the dryness amount is x = 0. CO_2 cycle pressure value was determined according to the values obtained from the literature review. According to these data, the necessary thermodynamic parameters at the 5^{th} point were calculated. As in the *SRC*, the pump outlet enthalpy was calculated according to the pump work and condenser outlet enthalpy in the CO_2 cycle. The CO_2 cycle *TIT* was determined according to the literature, and the turbine output power was calculated with the input parameters. The net power output of the combined system is 770.2 kW.

Mass flow rate has an essential effect on transferring heat taken from the flue gas to the *ORC*. The electricity generation cost obtained by parametric study of the mass flow rate from 2.75 kg/s to 18 kg/s is shown in Figure 6.5.

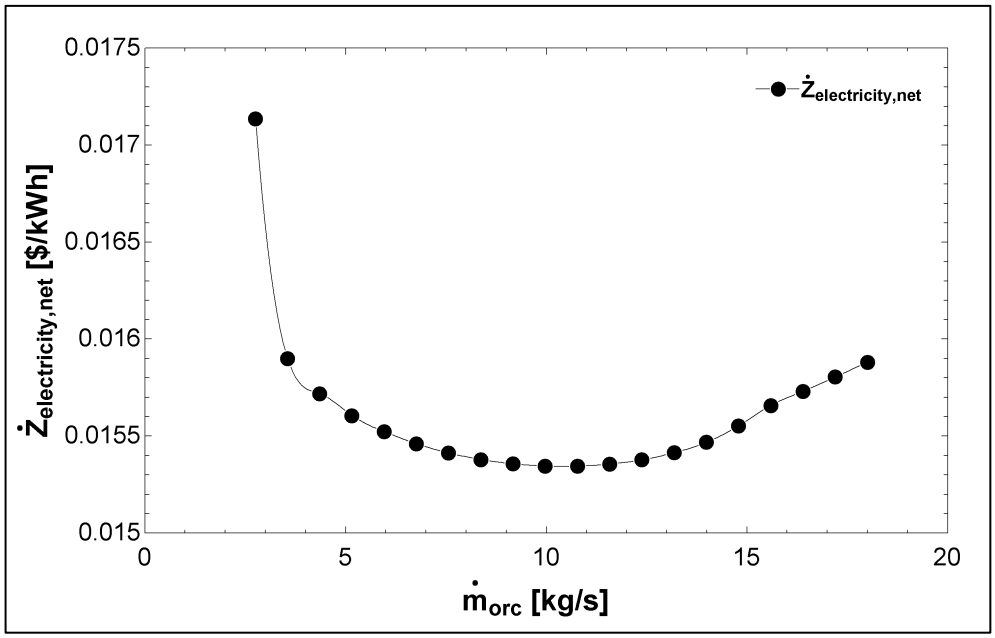

Figure 6.5. Variation of $\dot{Z}_{electricity}$ versus $\dot{m}_{orc}$.

Figure 6.6 indicates *TIT* of *ORC* decreased according to increasing mass flowrate from 1089 K to 395 K.

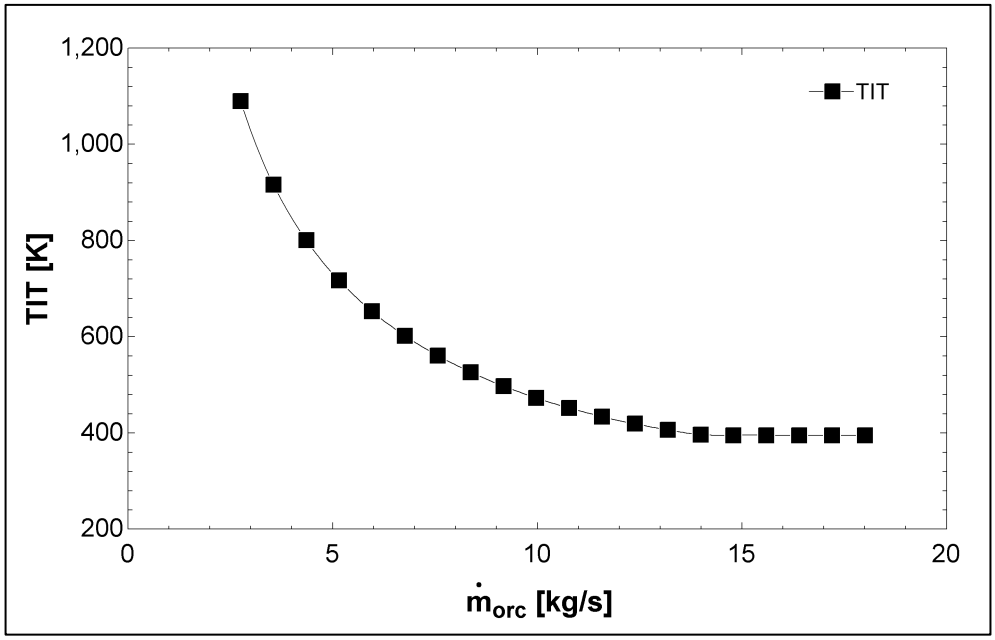

Figure 6.6. Effects of increasing mass flow rate on *TIT* of *ORC*.

The overall system's net power output and thermal efficiency are represented in Figure 6.7 according to the mass flow rate from 2.75 kg/s to 18 kg/s. *ORC* goes beyond the

operating temperature range of *R245fa* at mass flow rates less than 2.75 kg/s. The *ORC* does not work at mass flow rates more than 18 kg/s because the *R245fa* passes from the vapor phase to the liquid phase at the 11th point. The net power output of *ORC* increased from 456.9 kW to 598.7 kW according to the increasing mass flow rate. Unlike, the net power output of CO_2 cycle reduced from 125.9 kW to 120.1 kW. The higher net power output *ORC* than the CO_2 cycle total thermal efficiency and net power output changed from 0.16 and 582.8 kW to 0.20 and 718.8 kW, respectively. The optimum mass flow rate is 10.78 kg/s according to *R245fa* operating temperature for these combined system. Net power output, thermal efficiency and electricity generation cost are 766.2 kW, 0.21 and 0.01534 4 $/kWh due to mass flow rate.

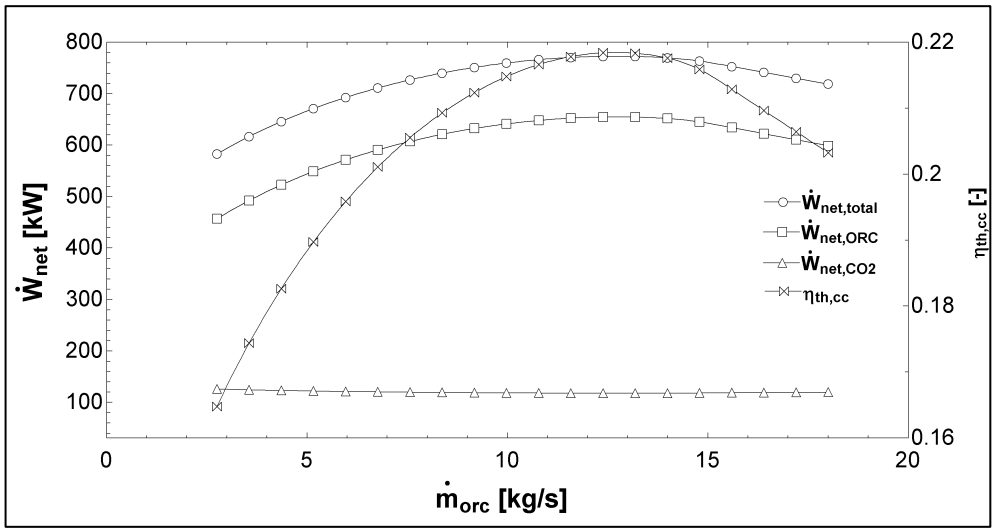

Figure 6.7. Variation of $\dot{W}_{net}$, $\dot{W}_{net,ORC}$, $\dot{W}_{net,CO2}$, $\eta_{th,cc}$.

For *ORC*-CO_2 combined system, to determine the minimum electricity generation cost, the parametrically studied mass flow rate values versus the thermal efficiency, net power output and *TIT* are shown as a summary Table 6.2. Figure 6.8 depicts the T-s diagram of *ORC* according to the optimum mass flow rate.

Table 6.2. Parametric results of *ORC-CO_2* combined system according to mass flow rate of *ORC*.

$\dot{m}_{orc}$ (kg/s)	η_{cc} (-)	$\dot{Z}_{electricity,net}$ ($/kWh)	$\dot{W}_{net,total}$ (kW)	TIT_{orc} (K)
2.75	0.1648	0.01714	582.8	1,089
3.553	0.1744	0.0159	616.8	915.8
4.355	0.1826	0.01572	646	800.2
5.158	0.1897	0.01561	671.1	716.6
5.961	0.1958	0.01552	692.7	652.7
6.763	0.2011	0.01546	711.2	601.9
7.566	0.2055	0.01541	727	560.6
8.368	0.2093	0.01538	740.2	526.2
9.171	0.2124	0.01536	751.1	497.2
9.974	0.2148	0.01535	759.7	472.6
10.78	0.2166	0.01534	766.2	451.7
11.58	0.2178	0.01536	770.4	433.9
12.38	0.2184	0.01538	772.5	418.8
13.18	0.2183	0.01541	772.2	406.3
13.99	0.2176	0.01547	769.7	396.3
14.79	0.2159	0.01555	763.5	395
15.59	0.2129	0.01566	752.9	395
16.39	0.2097	0.01573	741.5	395
17.2	0.2064	0.01581	730.2	395
18	0.2032	0.01588	718.8	395

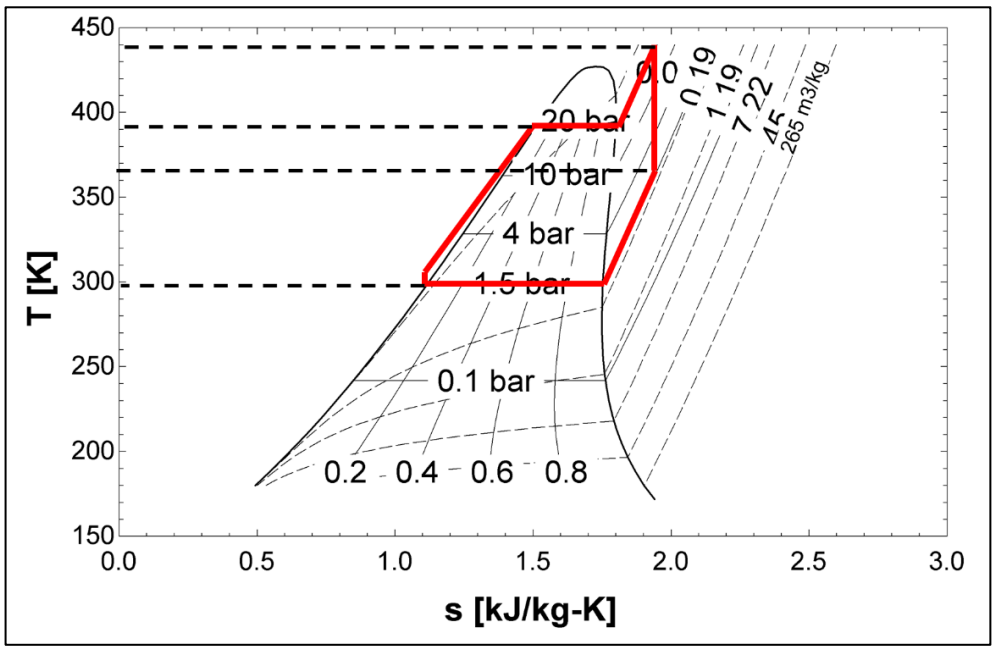

Figure 6.8. T-s diagram of *ORC*.

6.3. *KC-CO_2* COMBINED SYSTEM

The *KC* is optimized considering the minimum cost of electricity generation. Alteration of mass flow rate represented Figure 6.9 according to the *TIT* from 450 K to 490 K. The mass flowrate linearly reduced from 3.51 kg/s to 2.16 kg/s due to an increase in *TIT*.

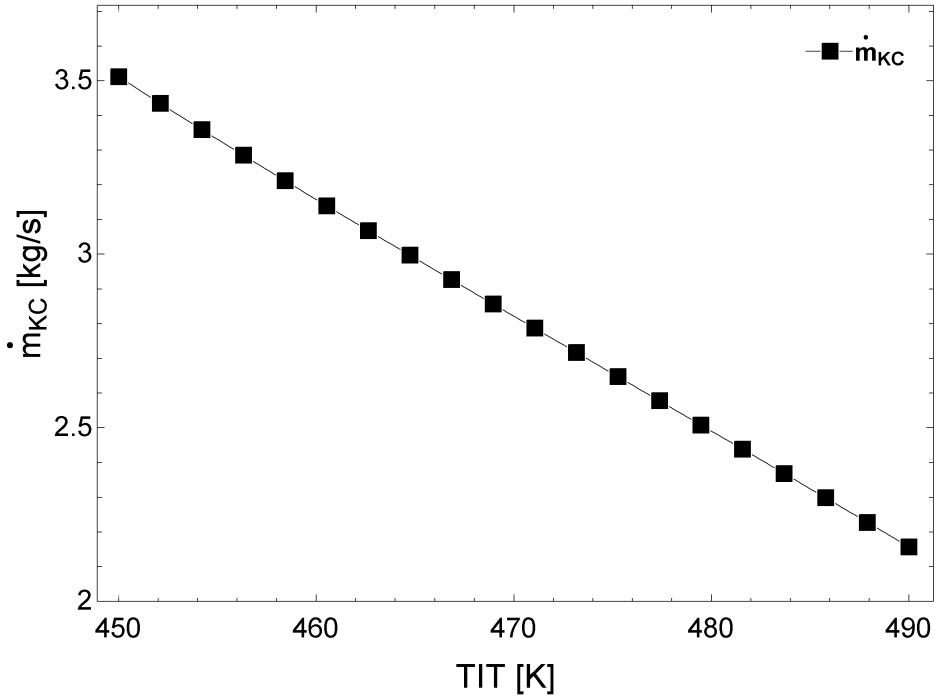

Figure 6.9. Variation of mass flow rate according to *TIT* of *KC*.

Net power output and thermal efficiency of combined system are represented in Figure 6.10 according to the *TIT* between 450 K, and 490 K. Net power output of *KC* increased from 631.9 kW to 831.1 kW according to increasing *TIT*. Similarly, the net power output of CO_2 cycle increased from 103.1 kW to 111.8 kW. The higher net power output *KC* than the CO_2 cycle total thermal efficiency and net power output increased from 0.20 and 735 kW to 0.26 and 942.9 kW, respectively.

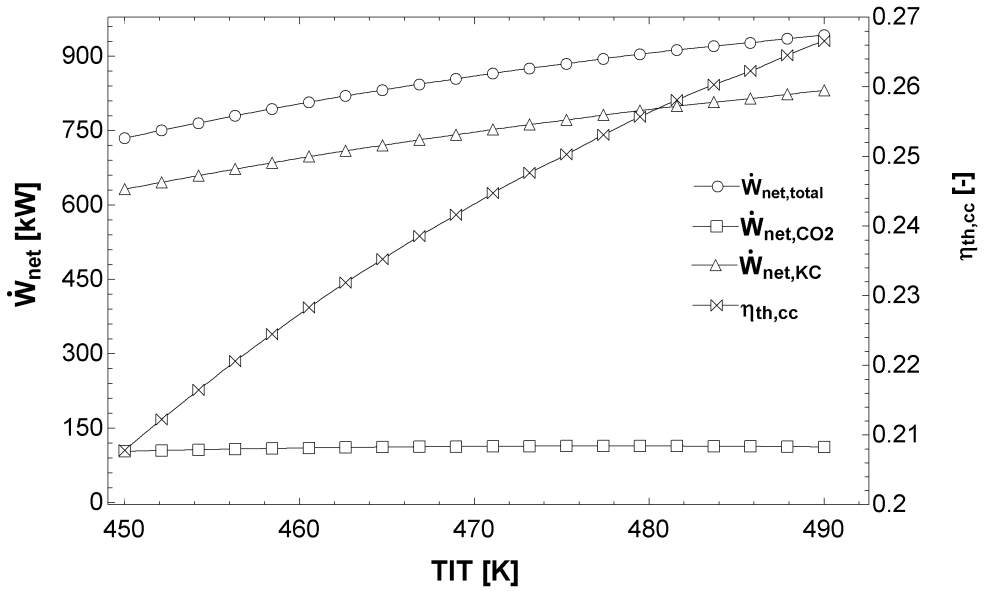

Figure 6.10. Variation of $\dot{W}_{net,total}$, $\dot{W}_{net,KC}$, $\dot{W}_{net,CO2}$, $\eta_{th,cc}$.

Figure 6.11 demonstrates the $\dot{Z}$ of the *KC-CO₂* combined system depending on the *TIT*. The cost of electricity generation is 0.08427 $/kWh for *TIT* of 487.9 K. While the $\dot{Z}$ decreases from 0.1118 $/kWh to 0.08427 $/kWh with the change of *TIT* between 450 K and 487.9 K, it increases from 0.08427 $/kWh to 0.08431 $/kWh between 487.9 K and 490 K. In consequence, for the minimum $\dot{Z}$, optimum values for *TIT*, net power output and thermal efficiency of combined system are determined as 487.9 K, 935.6 kW and 0.26, respectively.

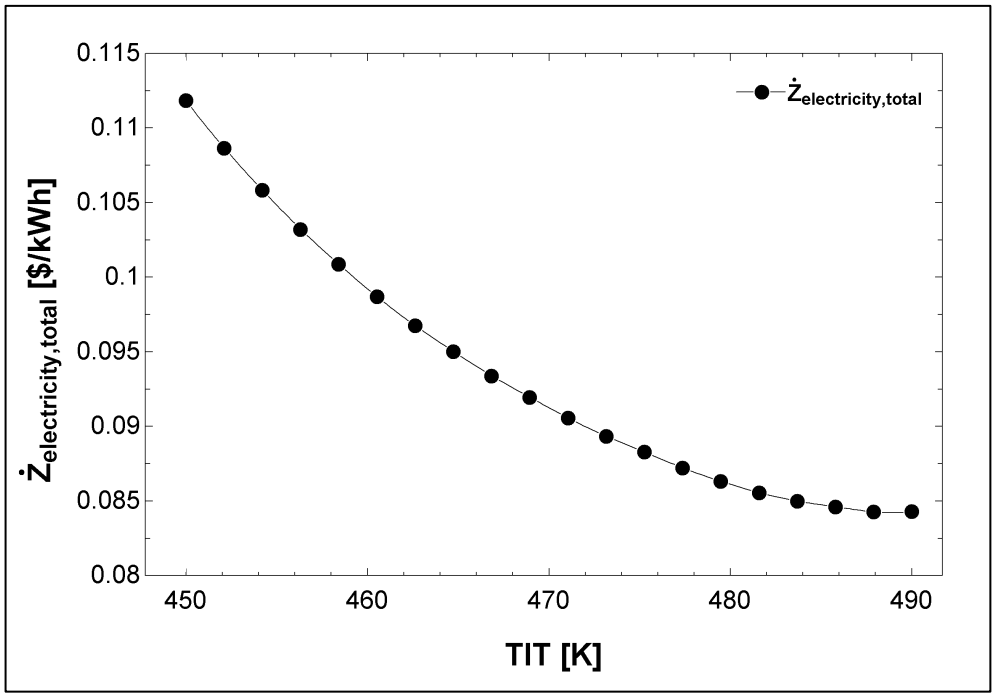

Figure 6.11. Variation of $\dot{Z}_{electricity,total}$ versus *TIT* of *KC*.

For *KC-CO₂* combined system, to determine the minimum electricity generation cost, the parametrically studied *TIT* values versus the thermal efficiency, net power output and *TIT* are shown as a summary Table 6.3.

Table 6.3. Parametric results of *KC-CO₂* combined system according to *TIT* of *KC*.

TIT_{kc} (K)	η_{cc} (-)	$\dot{W}_{net,total}$ (kW)	$\dot{Z}_{electricity,total}$ ($/kWh)	$\dot{m}_{kc}$ (kg/s)
450	0.2078	735	0.1118	3.511
452.1	0.2123	750.8	0.1087	3.434
454.2	0.2165	765.6	0.1058	3.359
456.3	0.2206	780.2	0.1032	3.285
458.4	0.2245	794.1	0.1009	3.212
460.5	0.2283	807.5	0.09869	3.139
462.6	0.2319	820.2	0.09675	3.068
464.7	0.2352	832.1	0.09502	2.997
466.8	0.2386	843.7	0.09339	2.927
468.9	0.2416	854.6	0.09195	2.856
471.1	0.2447	865.6	0.09056	2.787
473.2	0.2476	875.9	0.08934	2.717
475.3	0.2503	885.3	0.08828	2.647
477.4	0.2531	895.2	0.08722	2.578
479.5	0.2557	904.4	0.08631	2.508
481.6	0.2581	913	0.08556	2.438
483.7	0.2603	920.7	0.08498	2.368
485.8	0.2623	927.6	0.08461	2.298
487.9	0.2645	935.6	0.08427	2.227
490	0.2666	942.9	0.08431	2.157

6.4. *SRC-ORC-KC* COMBINED SYSTEM

In the combined system where all cycles are used, the inlet and outlet temperatures of the *SRC* evaporator were studied parametrically. The *ΔT* was initially set at 400. According to this temperature difference, the net power output obtained from the cycles is respectively 431.6 kW, 223.8 kW, 207.3 kW and 128.3 kW. Some thermodynamic parameters used in these cycles were determined as a result of a literature search. The input parameters of the *CO₂* cycle are assumed to be constant. The net power output was calculated with the mass flow changing due to the heat dissipated according to the previous cycle.Figure 6.12 depicts net power outputs and thermal efficiencies of each cycle according to ΔT between 300 K and 430 K. Net power output of *SRC* increased from 310 kW to 470.2 kW, the net power output of *CO₂* increased from 160.8 kW to 243.8 kW and net power output of *ORC* increased from 183.2 kW to 215.9 kW according to increasing *ΔT*. The net power output of the

combined system increased from 872 kW to 1025 kW. On the contrary, the net power output of *KC* decreased from 217.9 kW to 95.22 kW. The thermal efficiency of combined system decreased from 0.55 to 0.43.

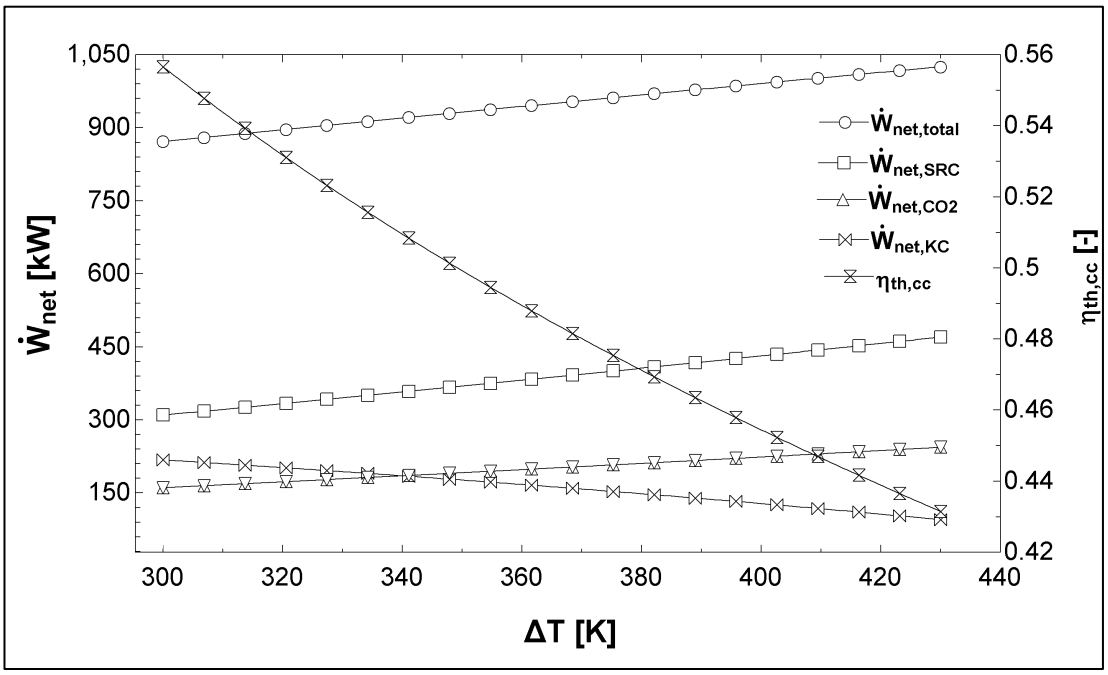

Figure 6.12. Variation of $\dot{W}_{net,total}$, $\dot{W}_{net,SRC}$, $\dot{W}_{net,ORC}$, $\dot{W}_{net,KC}$, $\dot{W}_{net,CO2}$, $\eta th,cc$.

Figure 6.13 represented the $\dot{Z}$ value of the combined system depending on the ΔT. The cost of electricity generation is 0.01706 $/kWh at ΔT of 416.3 K. $\dot{Z}$ value decreases from 0.01801 $/kWh to 0.01706 $/kWh and increases from 0.01706 $/kWh to 0.01711 $/kWh. Consequently, for the minimum $\dot{Z}$ value, optimum values for ΔT, net power output and thermal efficiency of combined system are determined as 416.3 K, 1010 kW and 0.44, respectively.

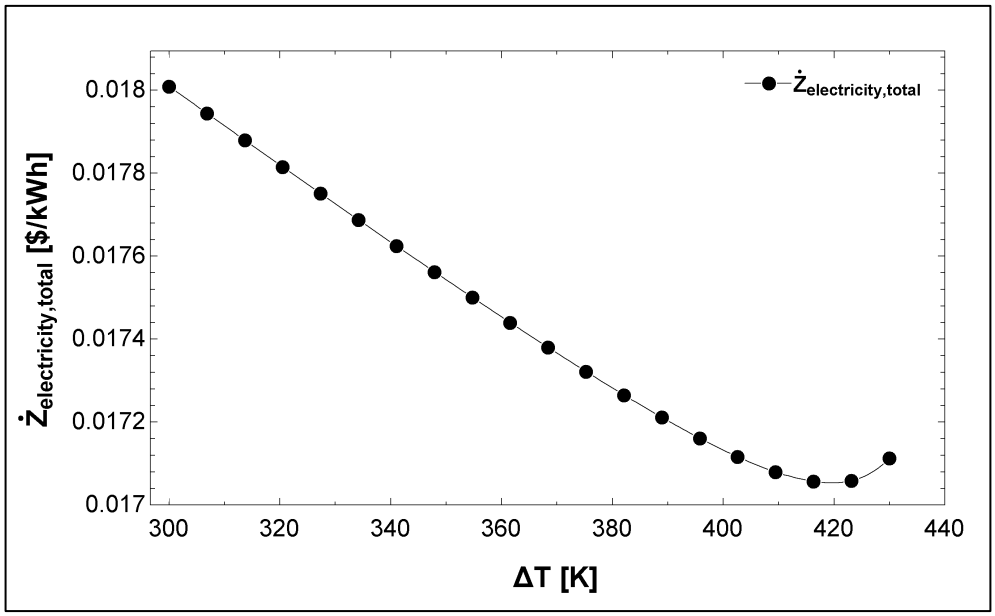

Figure 6.13. Variation of $\dot{Z}_{electricity,total}$ versus ΔT.

For *SRC-ORC-KC* combined systems, to determine the minimum electricity generation cost, the parametrically studied ΔT values versus the thermal efficiency, net power output are shown as a summary Table 6.4. Figure 6.14 represents the T-s diagram of CO_2 cycle.

Table 6.4. Parametric results of *SRC-ORC-KC* combined system according to *ΔT*.

ΔT	$\dot{Z}_{electricity,total}$ ($/kWh)	$\dot{W}_{net}$ (kW)	η_{cc} (-)
300	0.01801	872	0.5566
306.8	0.01794	880.2	0.5477
313.7	0.01788	888.4	0.5392
320.5	0.01782	896.7	0.5311
327.4	0.01775	904.9	0.5232
334.2	0.01769	913.1	0.5157
341.1	0.01762	921.3	0.5084
347.9	0.01756	929.5	0.5013
354.7	0.0175	937.6	0.4945
361.6	0.01744	945.8	0.4879
368.4	0.01738	953.9	0.4816
375.3	0.01732	962	0.4754
382.1	0.01727	970.1	0.4694
388.9	0.01721	978.1	0.4635
395.8	0.01716	986.1	0.4579
402.6	0.01712	994	0.4523
409.5	0.01708	1,002	0.4469
416.3	0.01706	1,010	0.4417
423.2	0.01706	1,017	0.4365
430	0.01711	1,025	0.4315

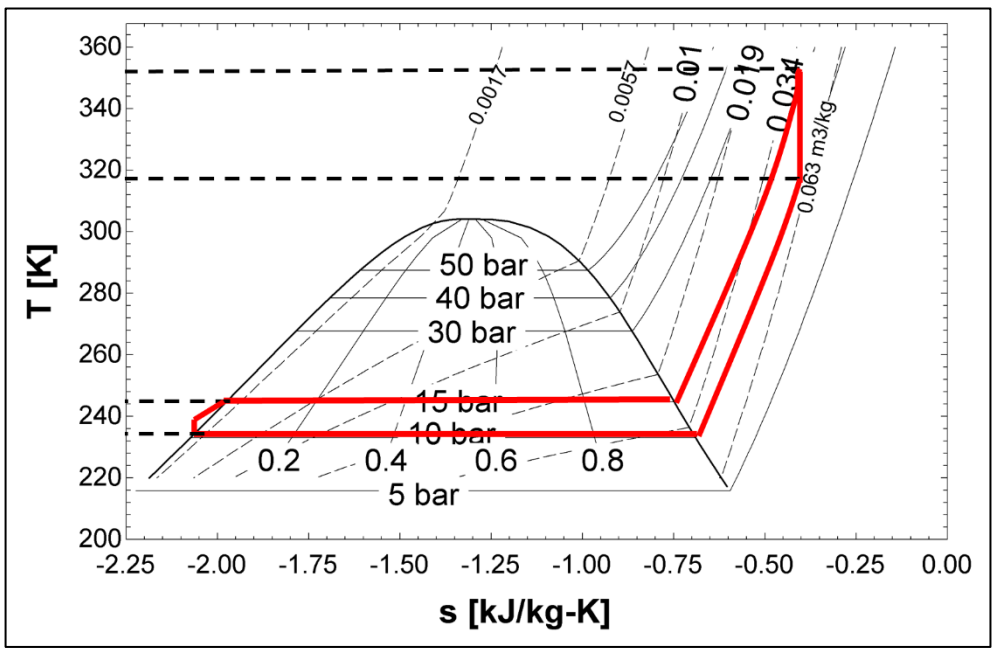

Figure 6.14. T-s diagram of CO_2.

The net power output of the *SRC-CO_2* combined system is 1274 kW, the thermal efficiency is 0.36, and the electricity generation cost is 0.01153 $/kWh at an optimum mass flow rate. The net power output of the *ORC-CO_2* combined system is 766.2 kW, the thermal efficiency is 0.21, and the electricity generation cost is 0.01534 $/kWh at an optimum mass flow rate. The net power output of the *KC-CO_2* combined system is 935.6 kW, the thermal efficiency is 0.26, and the electricity generation cost is 0.08427 $/kWh at an optimum mass flow rate. According to the optimum ΔT of the *SRC-ORC-KC* combined system, the net power output, thermal efficiency and electricity generation cost are 1010 kW, 0.44, and 0.01706 $/kWh, respectively. When all combined systems evaluated in terms of $\dot{W}_{net}$ for an optimum value, *SRC-CO_2* combined system showed the best result with a net power output of 1274 kW. *SRC-CO_2* combined system has a minimum electricity generation cost of 0.01153 $/kWh. When all combined systems are compared to thermal efficiency, *SRC-ORC-KC* combine system have the best result with the thermal efficiency of 0.44.

SECTION 7

CONCLUSION

In the current study, recovering options of the waste heat released into the atmosphere from an industrial annealing furnace using various integrated systems are aimed by Thermodynamics and thermoeconomic aspects. In addition, calculations were made in terms of CO_2 emission. The waste heat at 1093.15 K from the furnace, four different integrated systems were used. The mass flow rate of *SRC-*CO_2 combine system, *ORC-*CO_2 combine system studied parametrically. The *TIT* of *KC-*CO_2 and ΔT of *SRC-ORC-KC* combine system studied parametrically. As a result of the study, the systems were evaluated regarding thermal efficiency, investment cost and net output power. As a result of the study,

- The net power output from highest to lowest are 1294 kW (*SRC-*CO_2), 1010 kW (*SRC-ORC-KC*) 935.6 kW (*KC-*CO_2) and 766.2 kW (*ORC-*CO_2) when the powers from the combined cycles are compared with each other.

- The electricity generation cost from lowest to highest are 0.01153 $/kWh (*SRC-*$CO_2$), 0.01534 $/kWh (*ORC-*$CO_2$), 0.01706 $/kWh (*SRC-ORC-KC*) and 0.08427 $/kWh (*KC-*$CO_2$) when the electricity generation cost from the combined cycles are compared with each other.

- The thermal efficiency from highest to lowest are 0.44 (*SRC-ORC-KC*) 0.36 (*SRC-* CO_2), 0.26 (*KC-*CO_2) and 0.21 (*ORC-*CO_2) when the thermal efficiency from the combined cycles are compared each other.

- If we had produced the electricity generated from the system from a facility that produces electricity using natural gas, 2198 tons of CO_2 emissions would be released into the atmosphere.

- 4159 tons of CO_2 emissions would be released into the atmosphere if we had produced the electricity, we produced from the system from a facility that generates electricity using coke coal.

- Condensation in the condenser part of the cycles is provided by low operating temperature oxygen. This oxygen can be used in the melt shop section of the industrial facility.

REFERENCES

1. Kayabasi, E., "Experimental Analysis and Modeling of Photovoltaic Panels", ***Karabük University The Graduate School of Natural and Applied Sciences,*** Karabük**,** 10-20, (2018).

2. Eyidoğan, M., Kaya, D., Dursun, Ş., and Taylan, O., "Endüstriyel Tav Fırınlarında Enerji Tasarrufu ve Emisyon Azaltım Fırsatları", ***Journal Of The Faculty Of Engineering And Architecture Of Gazi University***, 29 (4): 735–743 (2014).

3. Pulat, E., Etemoglu, A. B., and Can, M., "Waste-heat recovery potential in Turkish textile industry: Case study for city of Bursa", ***Renewable And Sustainable Energy Reviews***, 13 (3): 663–672 (2009).

4. Kilinç, H., "Sanayide Atık Isı Geri Kazanımında Isı Değiştiricilerin Kullanılması", ***Tesisat Mühendisliği***, 71–73 (2016).

5. Ozcan, H. and Kayabasi, E., "Thermodynamic and economic analysis of a synthetic fuel production plant via CO2 hydrogenation using waste heat from an iron-steel facility", ***Energy Conversion And Management***, 236 (February): 114074 (2021).

6. Bakay, M. S. and Ağbulut, Ü., "Electricity production based forecasting of greenhouse gas emissions in Turkey with deep learning, support vector machine and artificial neural network algorithms", ***Journal Of Cleaner Production***, 285: 125324 (2021).

7. Ma, G. Y., Cai, J. J., Zeng, W. W., and Dong, H., "Analytical research on waste heat recovery and utilization of china's iron & steel industry", ***Energy Procedia***, 14: 1022–1028 (2012).

8. Zhao, J., Ma, L., Zayed, M. E., Elsheikh, A. H., Li, W., Yan, Q., and Wang, J., "Industrial reheating furnaces: A review of energy efficiency assessments, waste heat recovery potentials, heating process characteristics and perspectives for steel industry", ***Process Safety And Environmental Protection***, 147: 1209–1228 (2021).

9. Su, Z., Zhang, M., Xu, P., Zhao, Z., Wang, Z., Huang, H., and Ouyang, T., "Opportunities and strategies for multigrade waste heat utilization in various industries: A recent review", ***Energy Conversion And Management***, 229 (August 2020): 113769 (2021).

10. Pili, R., García Martínez, L., Wieland, C., and Spliethoff, H., "Techno-economic potential of waste heat recovery from German energy-intensive

industry with Organic Rankine Cycle technology", ***Renewable And Sustainable Energy Reviews***, 134 (February): 110324 (2020).

11. Wang, L., Bu, X., and Li, H., "Multi-objective optimization and off-design evaluation of organic rankine cycle (ORC) for low-grade waste heat recovery", ***Energy***, 203: 117809 (2020).

12. Zhang, X., He, M., and Zhang, Y., "A review of research on the Kalina cycle", ***Renewable And Sustainable Energy Reviews***, 16 (7): 5309–5318 (2012).

13. He, T. and Lin, W., "Energy saving research of natural gas liquefaction plant based on waste heat utilization of gas turbine exhaust", ***Energy Conversion And Management***, 225 (August): 113468 (2020).

14. Zhang, Q., Zhao, X., Lu, H., Ni, T., and Li, Y., "Waste energy recovery and energy efficiency improvement in China's iron and steel industry", ***Applied Energy***, 191: 502–520 (2017).

15. Ishaq, H., Dincer, I., and Naterer, G. F., "Exergy and cost analyses of waste heat recovery from furnace cement slag for clean hydrogen production", ***Energy***, 172: 1243–1253 (2019).

16. Köse, Ö., Koç, Y., and Yağlı, H., "Performance improvement of the bottoming steam Rankine cycle (SRC) and organic Rankine cycle (ORC) systems for a triple combined system using gas turbine (GT) as topping cycle", ***Energy Conversion And Management***, 211 (March): 112745 (2020).

17. Liu, X., Nguyen, M. Q., Chu, J., Lan, T., and He, M., "A novel waste heat recovery system combing steam Rankine cycle and organic Rankine cycle for marine engine", ***Journal Of Cleaner Production***, 265: 121502 (2020).

18. Zhang, X., Bai, H., Li, N., and Zhang, X., "Power generation by organic rankine cycle from low temperature waste heat of metallurgical industry", ***Energy Technology 2016: Carbon Dioxide Management And Other Technologies***, 57–64 (2016).

19. Song, J., Song, Y., and Gu, C. wei, "Thermodynamic analysis and performance optimization of an Organic Rankine Cycle (ORC) waste heat recovery system for marine diesel engines", ***Energy***, 82: 976–985 (2015).

20. Zare, V. and Mahmoudi, S. M. S., "A thermodynamic comparison between organic rankine and kalina cycles for waste heat recovery from the gas turbine-modular helium reactor", ***Energy***, 79 (C): 398–406 (2015).

21. Nemati, A., Nami, H., Ranjbar, F., and Yari, M., "A comparative thermodynamic analysis of ORC and Kalina cycles for waste heat recovery: A case study for CGAM cogeneration system", ***Case Studies In Thermal Engineering***, 9: 1–13 (2017).

22. Singh, O. K. and Kaushik, S. C., "Energy and exergy analysis and optimization of Kalina cycle coupled with a coal fired steam power plant", ***Applied Thermal***

Engineering, 51 (1–2): 787–800 (2013).

23. Emadi, M. A., Chitgar, N., Oyewunmi, O. A., and Markides, C. N., "Working-fluid selection and thermoeconomic optimisation of a combined cycle cogeneration dual-loop organic Rankine cycle (ORC) system for solid oxide fuel cell (SOFC) waste-heat recovery", ***Applied Energy***, 261 (August 2019): 114384 (2020).

24. Özahi, E., Tozlu, A., and Abuşoğlu, A., "Thermoeconomic multi-objective optimization of an organic Rankine cycle (ORC) adapted to an existing solid waste power plant", ***Energy Conversion And Management***, 168 (February): 308–319 (2018).

25. Nazari, N., Heidarnejad, P., and Porkhial, S., "Multi-objective optimization of a combined steam-organic Rankine cycle based on exergy and exergo-economic analysis for waste heat recovery application", ***Energy Conversion And Management***, 127: 366–379 (2016).

26. Chen, Z., Wang, Y., Zhang, X., and Xu, J., "The energy-saving mechanism of coal-fired power plant with S–CO2 cycle compared to steam-Rankine cycle", ***Energy***, 195: (2020).

27. Singh, A. and Singh, O., "Investigations on SOFC-HAT-sCO2 based combined power and heating cycle", ***Materials Today: Proceedings***, 38 (xxxx): 122–128 (2021).

28. Wang, F., Wang, L., Zhang, H., Xia, L., Miao, H., and Yuan, J., "Design and optimization of hydrogen production by solid oxide electrolyzer with marine engine waste heat recovery and ORC cycle", ***Energy Conversion And Management***, 229 (November 2020): 113775 (2021).

29. Liang, Y., Shu, G., Tian, H., and Sun, Z., "Investigation of a cascade waste heat recovery system based on coupling of steam Rankine cycle and NH3-H2O absorption refrigeration cycle", ***Energy Conversion And Management***, 166 (May): 697–703 (2018).

30. Mohammadi, K. and McGowan, J. G., "Thermodynamic analysis of hybrid cycles based on a regenerative steam Rankine cycle for cogeneration and trigeneration", ***Energy Conversion And Management***, 158 (January): 460–475 (2018).

31. Ghorbani, B., Ebrahimi, A., Rooholamini, S., and Ziabasharhagh, M., "Pinch and exergy evaluation of Kalina/Rankine/gas/steam combined power cycles for tri-generation of power, cooling and hot water using liquefied natural gas regasification", ***Energy Conversion And Management***, 223 (August): 113328 (2020).

32. Zhi, L. H., Hu, P., Chen, L. X., and Zhao, G., "Thermodynamic analysis of an innovative transcritical CO2 parallel Rankine cycle driven by engine waste heat and liquefied natural gas cold", ***Energy Conversion And Management***, 209 (December 2019): 112583 (2020).

33. Li, J., Li, P., Pei, G., Alvi, J. Z., and Ji, J., "Analysis of a novel solar electricity generation system using cascade Rankine cycle and steam screw expander", ***Applied Energy***, 165: 627–638 (2016).

34. Lu, F., Zhu, Y., Pan, M., Li, C., Yin, J., and Huang, F., "Thermodynamic, economic, and environmental analysis of new combined power and space cooling system for waste heat recovery in waste-to-energy plant", ***Energy Conversion And Management***, 226 (July): 113511 (2020).

35. Pan, M., Zhu, Y., Bian, X., Liang, Y., Lu, F., and Ban, Z., "Theoretical analysis and comparison on supercritical CO2 based combined cycles for waste heat recovery of engine", ***Energy Conversion And Management***, 219 (June): 113049 (2020).

36. Zhang, Q., Luo, Z., Zhao, Y., and Cao, R., "Performance assessment and multi-objective optimization of a novel transcritical CO2 trigeneration system for a low-grade heat resource", ***Energy Conversion And Management***, 204 (November 2019): 112281 (2020).

37. Mohammadi, Z., Fallah, M., and Mahmoudi, S. M. S., "Advanced exergy analysis of recompression supercritical CO2 cycle", ***Energy***, 178: 631–643 (2019).

38. Loni, R., Naja, G., Bellos, E., and Rajaee, F., "A review of industrial waste heat recovery system for power generation with Organic Rankine Cycle : Recent challenges and future outlook", ***Journal Of Cleaner Production***, (xxxx): (2020).

39. Fallah, M., Mahmoudi, S. M. S., Yari, M., and Ghiasi, R. A., "Advanced exergy analysis of the Kalina cycle applied for low temperature enhanced geothermal system", ***ENERGY CONVERSION AND MANAGEMENT***, 108: 190–201 (2016).

40. Wang, Y., Tang, Q., Wang, M., and Feng, X., "Thermodynamic performance comparison between ORC and Kalina cycles for multi-stream waste heat recovery", ***Energy Conversion And Management***, 143: 482–492 (2017).

41. Bahrampoury, R. and Behbahaninia, A., "Thermodynamic optimization and thermoeconomic analysis of four double pressure Kalina cycles driven from Kalina cycle system 11", ***Energy Conversion And Management***, 152 (September): 110–123 (2017).

42. Aghaziarati, Z. and Aghdam, A. H., "Thermoeconomic analysis of a novel combined cooling, heating and power system based on solar organic Rankine cycle and cascade refrigeration cycle", ***Renewable Energy***, 164: 1267–1283 (2021).

43. Ghaffarpour, Z., Mahmoudi, M., Mosaffa, A. H., and Garousi Farshi, L., "Thermoeconomic assessment of a novel integrated biomass based power generation system including gas turbine cycle, solid oxide fuel cell and Rankine cycle", ***Energy Conversion And Management***, 161 (November 2017): 1–12

(2018).

44. Sadeghi, M., Chitsaz, A., Marivani, P., Yari, M., and Mahmoudi, S. M. S., "Effects of thermophysical and thermochemical recuperation on the performance of combined gas turbine and organic rankine cycle power generation system: Thermoeconomic comparison and multi-objective optimization", ***Energy***, 210: 118551 (2020).

45. Khanmohammadi, S., Goodarzi, M., Khanmohammadi, S., and Ganjehsarabi, H., "Thermoeconomic modeling and multi-objective evolutionary-based optimization of a modified transcritical CO2 refrigeration cycle", ***Thermal Science And Engineering Progress***, 5 (July 2017): 86–96 (2018).

46. Ebadollahi, M., Rostamzadeh, H., Pedram, M. Z., Ghaebi, H., and Amidpour, M., "Proposal and multi-criteria optimization of two new combined heating and power systems for the Sabalan geothermal source", ***Journal Of Cleaner Production***, 229: 1065–1081 (2019).

47. Ayou, D. S. and Eveloy, V., "Energy, exergy and exergoeconomic analysis of an ultra low-grade heat-driven ammonia-water combined absorption power-cooling cycle for district space cooling, sub-zero refrigeration, power and LNG regasification", ***Energy Conversion And Management***, 213 (August 2019): 112790 (2020).

48. Seyyedvalilu, M. H., Zare, V., and Mohammadkhani, F., "Comparative thermoeconomic analysis of trigeneration systems based on absorption heat transformers for utilizing low-temperature geothermal energy", ***Energy***, 224: 120175 (2021).

49. Lu, F., Zhu, Y., Pan, M., Li, C., Yin, J., and Huang, F., "Thermodynamic, economic, and environmental analysis of new combined power and space cooling system for waste heat recovery in waste-to-energy plant", ***Energy Conversion And Management***, 226 (September): 113511 (2020).

50. Saadatfar, B., Fakhrai, R., and Fransson, T., "Exergo-environmental analysis of nano fluid ORC low-grade waste heat recovery for hybrid trigeneration system", ***Energy Procedia***, 61: 1879–1882 (2014).

51. Juhrich, K., "CO2 Emission Factors for Fossil Fuels", ***Climate Change***, 28: 45–47 (2016).

52. S.A. Klein, "Engineering Equation Solver", EES F-Chart, ***F-Chart Software***, Madison, 366 (2002).

RESUME

Her name is Büşra TOM. She won Karabük University Rail Systems Engineering Department in 2014 and Karabük University Mechanical Engineering Department with a double major program in 2016. She was in AEbt Angewandte Eisen Bahn Technik (Bavaria, Nuremberg, Germany) as an intern for 2017 summer break. In the summer holiday of 2018, Gökyapı San. Tic. Ltd. Şti. as an intern. She worked as a mechanical engineer in a company in 2019-2020. In 2019, she started her graduate education at Karabük University Graduate Education Institute, Department of Mechanical Engineering.